PEOPLE'S DEMOCRATIC REPUBLIC OF ALGERIA

MINISTRY OF HIGHER EDUCATION AND SCIENTIFIC RESEARCH

UNIVERSITY OF AMAR THELIDJI – LAGHOUAT

FACULTY: TECHNOLOGY

DEPARTEMENT: Mechanical Engineering

MASTER THESIS

DOMAIN: Science and Technology

FILIERE: Mechanical Engineering

OPTION: Energetic

Theme

Numerical Simulation of a Melting Problem by Electromagnetic Induction: Application on a Pure Tin

Prepared by: **BENAIDA Elhadj**

BENOUAR Omar Elfarouk

Juru of defense:

Full name	Grade	Quality
BENSAYAH Khaled	MCA	President
HAMDI Nassereddine	MAA	Examiner
HACHANI Lakhdar	Pr	Supervisor
ABDELHAKEM Abdelhafidh	Dr	Co-Supervisor

Promotion: June 2022

Dedication

To my dear **parents** who believe in me, and for all their sacrifices, their love, their support and their prayers throughout all my studies.

I say thank you **father** and **mother** for all what you have done for me, which allowed me to have this success.

To my dear brother and sisters, family and friends, for their support and encouragement.

To all those who have close place in my heart, family, friends and teachers for their support throughout my studies career.

Thank you all

Elhadj

Dedication

I dedicate this thesis to my parents

My mother, who has worked for my success, through her love, her support, her sacrifices and her precious advice, for all her assistance and presence in my life, receive through this work, the expression of my feelings and my eternal gratitude.

My father, who can be proud and find here the result of long years of sacrifices and hardships for helping me to advance in life. Thank you for the noble values, the education and the continuous support from you.

I dedicate this work to my dear family and friends who have always supported and encouraged me during the completion of this thesis, as well as to all those who are dear to me.

Thank you all

Farouk.

ACKNOWLEDGEMENTS

We are over helmed in all humbleness and gratefulness to acknowledge our depth to all those who have helped us to put these ideas, well above the level of simplicity and into something concrete.

we would like to express our special thanks of gratitude to all our teachers as well as our supervisor Pr.HACHANI Lakhdar and co-supervisor Dr.ADBELHAKEM Abdelhafidh those gave us the golden opportunity to do this wonderful project on the topic "Numerical simulation of electromagnetic induction melting", which also helped us in doing a lot of Research and we came to know about so many new things. We are really thankful to them.

Any attempt at any level can't be satisfactorily completed without the support and guidance of our parents, families and friends.

We would like to thank our parents who helped us a lot in gathering different information, collecting data and guiding us from time to time in making this project, despite of their busy schedules, they gave us different ideas in making this project unique.

Thank you,

BENAIDA Elhadj.

BENOUAR Omar El-Farouk.

Nomenclature

Latin symbols:

g	Acceleration due to gravity	m/s²
σ	Electrical conductivity	$\Omega^{-1}m^{-1}$
ρ_r	Electrical resistivity	$\Omega.m$
E	Energy	J
S	Entropy	J/K
F	Force	N
G	Gibbs free energy	J
q	Heat flux	W/m²
ϑ	Kinematic viscosity	m²/s
L	Latent heat	J
$\vec{F}$	Lorentz force	N/m^3
λ, η	Magnetic diffusivity	m²/s
$\vec{H}$	Magnetic field vector	A/m
μ	Magnetic permeability	H/m
m	Mass	Kg
δ	Porosity	g/cm^3
P_w	Power	W
P	Pressure force	Pa
R	Resistance	Ω
T	Temperature	K
t	Temps	S
τ_e	The charge relaxation time	F. Ω
I	The current	A
$\vec{J}$	The current density	A/m²
ρ	The density	kg/m^3
μ	The dynamic viscosity	kg/m.s
$\vec{E}$	The electric field	V/m
D	The electric induction	C/m²
φ	The electric potential	V
R_e	The electrical resistance	Ω
E_I	The internal energy	J
E_K	The kinetic energy	J
E_M	The magnetic energy	J
$\vec{B}$	The magnetic induction	T
C_p	The specific heat of constant pressure	J/kg.K
S, A	The surface	m²
$\boldsymbol{\lambda}$	The thermal conductivity	W/m.K
β	The thermal expansion coefficient	K^{-1}
$\vec{u}$	The velocity field	m/s
α	Thermal diffusivity	m²/s
Q	Thermal energy	W

$\overrightarrow{B_0}$	Uniform magnetic induction	T
ε_0	Vacuum permittivity	F/m
$\vec{V}$	Velocity	m/s
V	Voltage	V
R_e	Reynolds number	
P_r	Prandtl number	
G_r	Grashof number	
i	Index refers to the x-axis	
j	Index refers to the y-axis	
C	Constant	
x, y, z	Cartesian coordinates	
r, θ, z	Cylindrical coordinates	

Table of Contents

List of Figures

List of Tables

General Introduction:

Induction heating is widely used in metal industry because of its good heating efficiency, high production rate, and clean working environments. The development of high-frequency power supplies provided means of using induction furnaces for melting metals in continuous casting plants. The process of melting of both pure metals and metallic alloys is always accompanied by a set of hydrodynamic movements in the liquid phase, combined with heat and mass transfer which take place in the liquid and solid zones and in a particular way at the interface liquid-solid. The understanding of these physical phenomena is capital importance, because it makes it possible to better understand the process of phase change which is at the origin of the final structure of the material, and therefore of its mechanical characteristics. Flows in the liquid phase are mainly caused by the effect of thermosolutal convection due to a heterogeneous distribution of temperature fields and species in the case of alloys, and then we speak of thermosolutal convection.

This work is essentially based on the study the melting process by induction heating of pure metal (Tin) in terms of thermal field, dynamics and evolution of the melting front. To do this, an unsteady axisymmetric 2D two-phase numerical model based on the resolution of Maxwell's equations, fluid mechanic, energy, and phase change, was developed to simulate the fusion phenomenon by Joule effect with the variation of several parameters.

This work will be presented in three parts:

The first chapter recalls the fundamental notions of induction heating by Joule effect. It also allows to put a general synthesis on the governing equations of electromagnetic induction called Maxwell's equation in order to identify the main electromagnetic factors that have a direct effect on the driving of this process.

The second chapter allows to pose the governing notions of phase change phenomenon, namely the melting, in order to establish the basic details on which the rest of the work will be built. It will also make it possible to make a brief inventory of the subject studied, the models of equations and the interest shown in the process of the phenomenon of melting.

The third chapter describes the model established to simulate the melting phenomenon for the case of this pure metal chosen (Tin), the different equations used as well as the modifications introduced. This chapter will also present the results obtained through the numerical simulation implemented under the commercial software COMSOL Multiphysics. Several aspects will be discussed: dynamic thermal and morphology of the melting front.

Finally, a general ***conclusion*** underlines the major results brought by this master's work, and we end by giving some envisaged perspectives in the light of the results obtained within the framework of our work.

Chapter one:

Bibliographic search of electromagnetic induction heating

I. Bibliographic search of electromagnetic induction heating:

Induction heating is a process which is used to bond, harden or soften metals or other conductive materials. For many modern manufacturing processes, induction heating offers an attractive combination of speed, consistency and control. In the most common heating methods, a torch or open flame is directly applied to the metal part. But with induction heating, heat is actually "induced" within the part itself by circulating electrical currents.

It has made it possible to locate operations, such as hardening, in production lines along with other machine tools instead of in remote separate departments. This saves the time of transporting parts from one part of the factory to another. Induction heating is clean, it does not throw off unpleasant heat. Hence, working conditions around its machines are satisfying, and comparable to those around other modern metal-working machine tools. They do not give off the smoke and dirt which are sometimes associated with heat-treating departments and forge shops. [1]

Induction heating relies on the unique characteristics of radio frequency (RF) energy - that portion of the electromagnetic spectrum below infrared and microwave energy. Since heat is transferred to the product via electromagnetic waves, the part never comes into direct contact with any flame, the inductor itself does not get hot *Fig.I.1*, and there is no product contamination. When properly set up, the process becomes very repeatable and controllable.

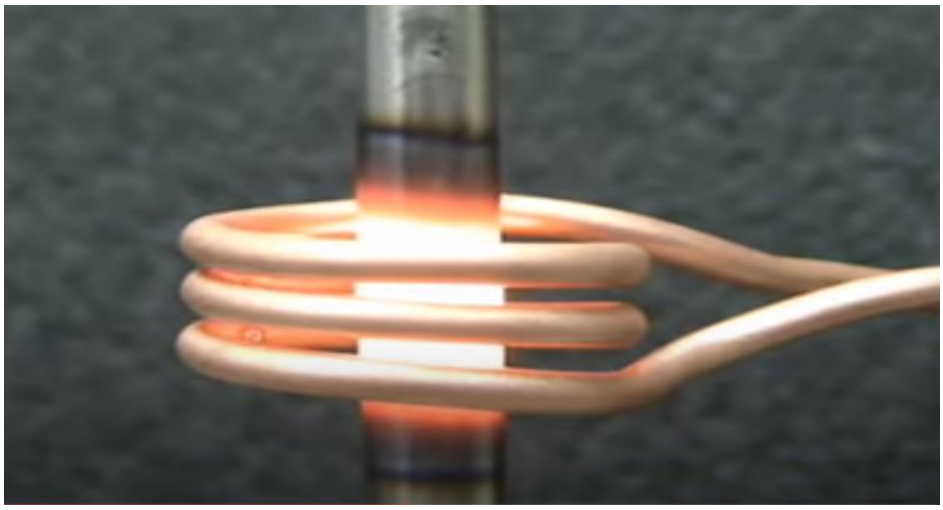

Fig.I.1. *shows how the part never touches the inductor coil [2].*

There are many production applications of induction heating, all these applications are not automatic, and do not involve high production. An example is the wide-spread use of induction for melting. Special alloy, both ferrous and non-ferrous are brewed in induction melting furnaces. The flexibility and clean-lines of induction melting cannot be duplicated by conventional steel mill and foundry methods. [1]

I.1. Joule heating effect:

The heating effect was first studies and characterized by the scientist James Prescott Joule, around the year *1840*. Joule heating is the physical effect by which the pass of current through an electrical conductor produces thermal energy. This thermal energy is then evidenced through a rise in the conductor material temperature, thus the term heating. One can see Joule heating as a transformation between electrical energy and thermal energy, following the energy conservation principal.

Joule heating of materials is used extensively in many applications in the industry products, transportation, or even at home. In the incandescent light, we can observe an amount of heat emit by their filament.

The power P absorbed in an electrical resistor of resistance R, current I, and voltage V is given by $P = I^2 \times R = \frac{V^2}{R} = V \times I$. Despite the fact that it has units of power, it is commonly referred to as joule heat. A given amount of electrical energy absorbed in the resistor (in units of joules) produces a fixed amount of heat (in units of calories). The constant ratio between the two has the value $4.184\ J/cal$ and is numerically equivalent to the specific heat capacity of water. [3]

When a resistor of resistance R has a current I at voltage V, the power absorbed in the resistor is

$$\boldsymbol{P = I^2 \times R = \frac{V^2}{R} = V \times I} \qquad \textbf{(I.1)}$$

Power is energy per unit time, and if the power is constant, the energy E delivered in time t is given by:

$$\boldsymbol{E = P \times t} \qquad \textbf{(I.2)}$$

Substituting *Eq. (I.1)* into *Eq. (I.2)* gives the following expression for the electrical energy:

$$\boldsymbol{E = V \times I \times t} \qquad \textbf{(I.3)}$$

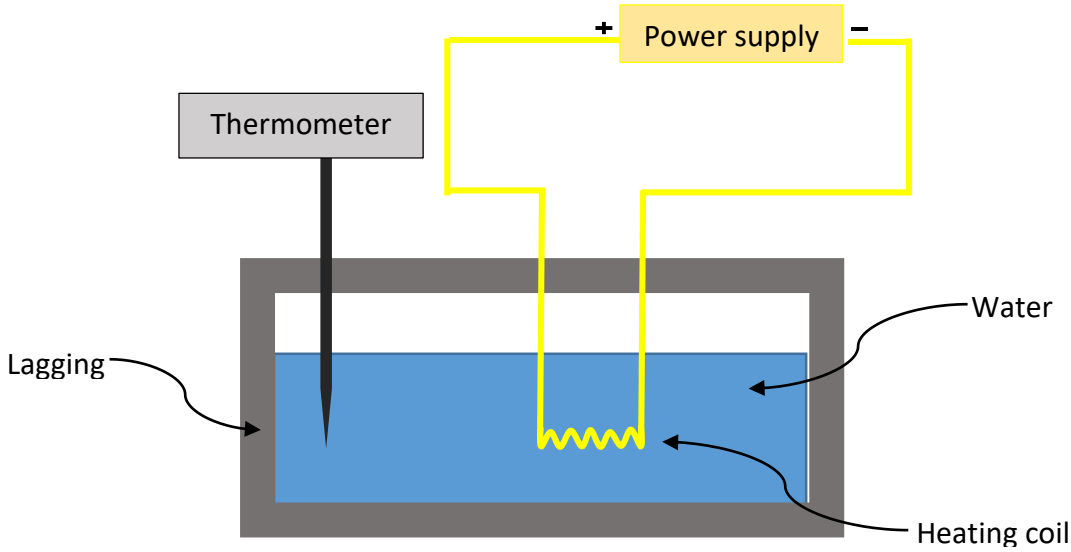

Fig.I.2. *Experimental arrangement and circuit diagram for the calorimetric measurement of the heat produced in an immersion heater by an electrical current.*

When a resistor absorbs electrical energy, it dissipates this energy in the form of heat Q. If the resistor is placed in the calorimeter, the amount of heat produced can be measured when it is absorbed in the calorimeter. Consider the experimental arrangement shown in *Fig.I.2*, which a resistor coil (also called and "*immersion heater*") is immersed in the water in a calorimeter. The heat Q produced in the resister is absorbed by the water, calorimeter cup, and the resistor coil itself. This heat Q produces a rise in temperature ΔT. [3],

The heat Q is related to ΔT by:

$$\boldsymbol{Q = (m_w Cp_w + m_c Cp_c + m_r Cp_r) \times \Delta T} \quad \textbf{(I.4)}$$

I.2. Overview of electromagnetism:

I.2.1. The electric field and the Lorentz forces:

A particle moving with velocity u and carrying a charge q is, in general, subject to three electromagnetic forces:

$$\boldsymbol{F = qE_s + qE_i + qu \times B} \quad \textbf{(I.5)}$$

The first is the electrostatic force, or Coulomb force, which arises from the mutual repulsion or attraction of electric charges (E_s is the electrostatic field). The second is the force which the charge experiences in the presence of a time-varying magnetic field, E_i being the electric field induced by the changing magnetic field. The third contribution is the Lorentz force which arises from the motion of the charge in a magnetic field, now Coulomb's law tells us that E_s is irrotational, and Gauss's law fixes the divergence of E_s. Together these laws yield, [4]

$$\boldsymbol{\vec{\nabla}.\overrightarrow{E_s} = \frac{\rho_e}{\varepsilon_0}} \quad \textbf{(I.6)}$$

$$\boldsymbol{\vec{\nabla}.\overrightarrow{E_s} = 0} \quad \textbf{(I.7)}$$

Here ρ_e is the total charge density (free charges plus bound charges) and ε_0 is the permittivity of free space. In *Eq. (I.7)*, we may introduce the electrostatic potential, V defined by $E_s = -\nabla.V$. It follows from *Eq. (I.6)*, that $\nabla^2 V = -\frac{\rho_e}{\varepsilon_0}$.

The induced electric field, on the other hand, has zero divergence, while its curl is finite and governed by Faraday's law

$$\boldsymbol{\vec{\nabla}.\overrightarrow{E_i} = 0 \quad \vec{\nabla}.\overrightarrow{E_i} = -\frac{\partial \vec{B}}{\partial t}} \quad \textbf{(I.8)}$$

It is convenient to define the total electric field as $E = E_s + E_i$ and so we have

Gauss's law:

$$\boldsymbol{\vec{\nabla}.\vec{E} = \frac{\rho_e}{\varepsilon_0}} \quad \textbf{(I.9)}$$

Faraday's law:

$$\vec{\nabla} \times \vec{E} = -\frac{\partial \vec{B}}{\partial t} \quad \textbf{(I.10)}$$

Electrostatic force plus Lorentz force:

$$\vec{F} = q(\vec{E} + \vec{u} \times \vec{B}) \quad \textbf{(I.11)}$$

Eq. (I.9) and *Eq. (I.10)* uniquely determine the electric field since the requirements are that the divergence and curl of the field be known (and suitable boundary conditions are specified). It is customary to use *Eq. (I.11)* to define the electric field $E$and the magnetic field B.thus, for example the electric field E is the force per unit charge on a small test charge at rest in the observer's frame of reference. [4]

Due attention must be given to frames of reference. Suppose that in the laboratory frame there is an electric field and a magnetic field. The electric field E, is defined by the force per unite charge on a charge at rest in the frame. If the charge is moving, the force due to the electric field is still given by $F = qE$ but the additional force $qu \times B$ appears, which is used to define B. If, however, we use a frame of reference in which the charge is instantaneously at rest (but moving with velocity u relative to the laboratory frame), than the force on the charge can only be interpreted as due to an electric field, say Er (the subscript r indicates 'relative to a moving frame'). Newton's second law than gives, for the two frames, $F = q(E + u \times B)$ and $Fr = qEr$. However, Newtonian relativity (which is all that is required for MHD) tells us that $F = Fr$ .It follows that the electric field in the two frames are related by

$$\overrightarrow{Er} = \vec{E} + \vec{u} \times \vec{B} \quad \textbf{(I.12)}$$

I.2.2. Ohm's law and the volumetric Lorentz force:

In a stationary conductor it is found that the current density J, is proportional to the force experienced by the free charges, this is reflected in the conventional from of Ohm's law $J = \sigma E$. In a conducting fluid the same law applies, only now we must use the electric field measured in a frame moving with the local velocity of the conductor

$$\vec{J} = \sigma \overrightarrow{E_r} = \sigma(\vec{E} + \vec{u} \times \vec{B}) \quad \textbf{(I.13)}$$

Note in general that u will vary with position.

Now the Lorentz force *Eq. (I.11)* is important not just because it lies behind Ohm's law, but also because the forces exerted on the free charges are ultimately transmitted to the conductor. In MHD we are less concerned with the forces on individual charges than the bulk force acting on the medium, but this is readily found. If *Eq. (I.11)* is summed over a unit volume of the conductor then $\sum q$ becomes the charge density ρ_e and $\sum qu$ becomes the current density J the volumetric version of *Eq. (I.11)* is therefore

$$\vec{F} = \rho_e(\vec{E} + \vec{u} \times \vec{B}) \quad \textbf{(I.14)}$$

Where F is the force per unit volume acting on the conductor. However, in conductors travelling at the sort of speeds we are interested in (much less than the speed of light), the first term in *Eq. (I.14)* is negligible. We may demonstrate this as follows. Conservation of charge requires that

$$\vec{\nabla}.\vec{J} = -\frac{\partial \vec{\rho_e}}{\partial t} \qquad \textbf{(I.15)}$$

(This simply says that the rate at which charge is decreasing inside a small volume must equal the rate at which charge flows out across the surface of that volume). By taking the divergence of both sides of *Eq. (I.13),* and using Gauss's law and *Eq. (I.15),* we find that

$$\frac{\partial \rho_e}{\partial t} + \frac{\rho_e}{\tau_e} + \sigma\vec{\nabla}.\left(\vec{u} \times \vec{B}\right) = 0, \quad \tau_e = \frac{\varepsilon_0}{\sigma}$$

The quantity τ_e is called the charge relaxation time, and for a typical conductor has a value of around $10^{-18}\ s$. It is extremely small! To appreciate where its name comes from, consider the situation where $u = 0$. In this case, $\frac{\partial \rho_e}{\partial t} + \frac{\rho_e}{\tau_e} = 0$ and so

$$\rho_e = \rho_e(0)\exp[-\frac{t}{\tau_e}]$$

Any net charge density which, at $t = 0$, lies in the interior of a conductor will move rapidly to the surface under the action of the electrostatic repulsion forces. It follows that ρ_e is always zero in stationary conductors, except during some minuscule period when a battery, say, is turned on. [4]

Now consider the case where u is non-zero. We are interested in events which take place on a time-scale much longer than τ_e (we exclude events like batteries being turned on) and so we may neglect $\frac{\partial \rho_e}{\partial t}$ by comparison with $\frac{\rho_e}{\tau_e}$. We are left with pseudo-static equation

$$\boldsymbol{\rho_e = -\varepsilon_0\vec{\nabla}.\left(\vec{u} \times \vec{B}\right)} \qquad \textbf{(I.16)}$$

Thus, when there is motion, we can sustain a finite charge density in the interior of the conductor. However, it turns out that ρ_e is very small, i.e., too low to produce any significant electric force $\rho_e E$. That is, from *Eq. (I.16)* we have $\rho_e \sim \frac{\varepsilon_0 uB}{l}$, while Ohm's law requires $E \sim \frac{J}{\sigma}$, and so

$$\rho_e E \sim \left[\frac{\varepsilon_0 uB}{l}\right]\left[\frac{J}{\sigma}\right] \sim \frac{u\tau_e}{l}JB$$

Here l is a typical length-scale for the flow. Evidently, since $\frac{u\tau_e}{l} \sim 10^{-18}$, the Lorentz force completely dominates *Eq. (I.14)* and we may write:

$$\vec{F} = \vec{J} \times \vec{B} \qquad \textbf{(I.17)}$$

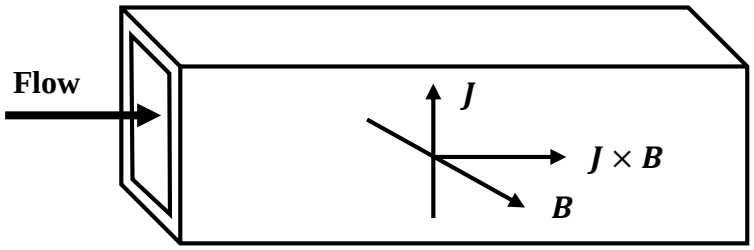

Fig.I.3. *the electromagnetic pump.*

Note also that *Eq. (I.16)* is equivalent to ignoring $\frac{\partial \rho_e}{\partial t}$ in the charge conservation equation *Eq. (I.15).*

That is to say, the charge density is so small that *Eq. (I.15)* simplifies to

$$\vec{\nabla}.\vec{J} = 0 \qquad \textbf{(I.18)}$$

I.2.3. Faraday's law in differential form:

Faraday's law is sometimes states in integral form and sometimes in differential form. You have already met both. $\vec{\nabla} \times \vec{E} = -\frac{\partial \vec{B}}{\partial t}$

This tells us about the electric field induced by a time-varying magnetic field.

$$e.m.f = \oint_c E_r.dl = -\frac{d}{dt}\int_S B.dS \qquad \textbf{(I.19)}$$

Where E_r is the electric field measured in a frame of reference moving with dl (see *Eq. (I.12)*). In fact, it is easily seen that *Eq. (I.19)* is a more powerful statement than the differential form of Faraday's law. In words, it states that the emf. round a closed loop is equal to the total rate of change of flux of B through that loop. In *Eq. (I.19),* the flux may change because B is changing with time, or because the loop is moving uniformly in an inhomogeneous field, or because the loop is changing shape. Whatever the cause *Eq. (I.19)* gives the induced emf. We shall return to the integral version of Faraday's law, where we discuss its full significance. In the meantime, we shall show that the differential form of Faraday's law is a special case of *Eq. (I.19).* [4]

Suppose, that the loop is rigid and at rest in a laboratory frame. Then the emf. can arise only from a magnetic field which is time-dependent. In this case *Eq. (I.19)* becomes,

$$\oint_c E.dl = \oint_s (\nabla \times E).dS = -\int_s \left(\frac{\partial B}{\partial t}\right).dS \qquad \textbf{(I.20)}$$

Since this is true for any and all (fixed) surfaces, we may equate the integrands in the surface integrals. We then obtain the differential form of Faraday's law

$$\vec{\nabla} \times \vec{E} = -\frac{\partial \vec{B}}{\partial t} \qquad \textbf{(I.21)}$$

In this form, Faraday's law becomes one of Maxwell's equations. Note, however, that *Eq. (I.21)* is a weaker statement than *Eq. (I.19).* It only tells us about the electric field induced by a time-varying magnetic field.

Now *Eq. (I.21)* ensures that $\frac{\partial \vec{B}}{\partial t}$ is solenoid, since $\vec{\nabla}.(\vec{\nabla} \times \vec{\mathrm{E}}) = 0$. In fact, it transpires that we can make an even stronger statement about B. It turns out that B is itself solenoidal

$$\vec{\nabla}.\vec{\mathbf{B}} = \mathbf{0} \qquad \textbf{(I.22)}$$

This allows us to introduce another field, A called the vector potential, and defined by

$$\vec{\nabla} \times \vec{\mathbf{A}} = \vec{\mathbf{B}} \qquad \textbf{(I.23)}$$

$$\vec{\nabla}.\vec{\mathbf{A}} = \mathbf{0} \qquad \textbf{(I.24)}$$

This definition automatically ensures that B is solenoidal, since $\vec{\nabla}.\vec{\nabla} \times \vec{\mathrm{A}} = 0$.if we substitute for A in Faraday's equation we obtain

$$\vec{\nabla} \times \vec{\mathrm{E}} = -\vec{\nabla} \times \frac{\partial \vec{A}}{\partial t}$$

From which

$$\vec{\mathbf{E}} = -\frac{\boldsymbol{\partial \vec{A}}}{\boldsymbol{\partial t}} - \vec{\nabla}\vec{\mathbf{V}} \qquad \textbf{(I.25)}$$

Where V is an arbitrary scale function. However, we also have, from *Eq. (I.6), Eq. (I.7)* and *Eq. (I.8)*

$$\vec{E} = \overrightarrow{E_\iota} + \overrightarrow{E_s} \quad \vec{\nabla}.\overrightarrow{E_s} = 0 \quad \vec{\nabla}.\overrightarrow{E_\iota} = 0$$

And so, we might anticipate that $\overrightarrow{E_\iota} = -\frac{\partial \vec{A}}{\partial t}$ and $\overrightarrow{E_s} = \vec{\nabla}\vec{\mathrm{V}}$ where V is now the electrostatic potential. This is readily confirmed by taking the divergence of *Eq. (I.20),* as required by *Eq. (I.6), Eq. (I.7)* and *Eq. (I.8).*

I.2.4. The reduced form of Maxwell's equations for MHD:

We have mentioned Maxwell's equations several times. When combined with the forces law *Eq. (I.11)* and the law of charge conservation *Eq. (I.15),* they embody all that we know about electrodynamics, and so it seems appropriate that, at some point, we should write them down. For materials which are neither magnetic nor dielectric, Maxwell's equations state that

Gauss's law: $\vec{\nabla}.\vec{\mathrm{E}} = \frac{\rho_e}{\varepsilon_0}$

Solenoid nature of B: $\vec{\nabla}.\vec{\mathrm{B}} = 0$

Faraday's law in differential form $\vec{\nabla} \times \vec{\mathrm{E}} = -\frac{\partial \vec{B}}{\partial t}$

In addition, we have

Charge conservation $\vec{\nabla}.\vec{\mathrm{J}} = 0$

$$\vec{F} = q(\vec{E} + \vec{u} \times \vec{B})$$

For our purposes these may be simplified considerably. In MHD, the charge density ρ_e plays no significant part. For example, we have seen that the electric forces qE, is minute by comparison with the Lorentz forces, and that the contribution of $\frac{\partial \rho_e}{\partial t}$ to the charge conservation equation is also negligible. Apparently ρ_e is significant only in Gauss's law and so we simply drop Gauss's law and ignore ρ_e. Also, we have seen that in MHD the displacement currents are negligible by comparison with the current density J, and so the Ampere-Maxwell equation reduces to the differential form of Ampere's law. We may now summarize the (pre-Maxwell) form of the electrodynamics equations used in MHD, [4]

Ampere's law plus charge conservation:

$$\vec{\nabla} \times \vec{\mathbf{B}} = \mu\vec{J} \quad \vec{B} = \mu\vec{H} \quad \vec{\nabla}.\vec{\mathbf{J}} = \mathbf{0} \qquad \textbf{(I.26)}$$

Faraday's law plus the solenoid constraint on B,

$$\vec{\nabla} \times \vec{\mathbf{E}} = -\frac{\partial \vec{B}}{\partial t} \quad \vec{\nabla}.\vec{\mathbf{B}} = \mathbf{0} \qquad \textbf{(I.27)}$$

Ohm's law plus the Lorentz forces:

$$\vec{J} = \sigma(\vec{E} + \vec{u} \times \vec{B}) \qquad \vec{\mathbf{F}} = \vec{\mathbf{J}} \times \vec{\mathbf{B}} \qquad \textbf{(I.28)}$$

Eq. (I.26), Eq. (I.27) and *Eq. (I.28)* encapsulate all that we need to know about electromagnetism for MHD.

I.3. Basic electromagnetic phenomena in induction heating:

The basic electromagnetic phenomena of induction heating are quite simple. An alternating voltage applied to an induction coil (e.g.., solenoid coil) will result in an alternating current in the coil circuit. An alternating coil current will produce in its surroundings a time- variable magnetic field that has the same frequency as the coil current. This magnetic field induces eddy currents in the work-piece located inside the coil. Eddy currents will also be induced in other electrically conductive objects that are located near the coil. These induced currents have the same frequency as the coil current; however, their direction is opposite to the coil current. These currents produce heat by the Joule effect ($I^2 \times R$). [5]

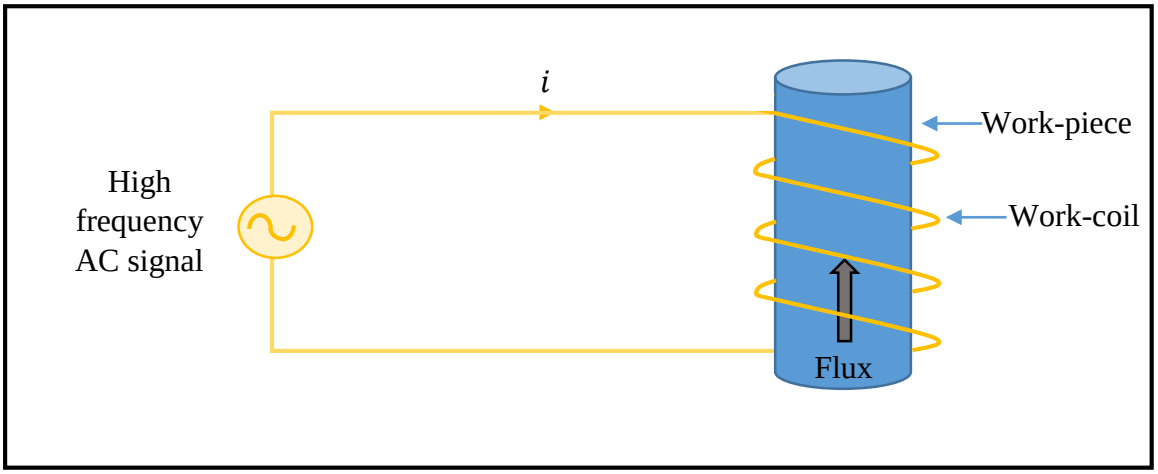

Fig.I.4. *set-up for induction heating.*

A conventional induction heating system that consists of a cylindrical load surrounded by a multi turn induction coil is shown in the *Fig.I.4.* Because of several electromagnetic phenomena, the current distribution within an inductor and work-piece is not uniform. This heat source non-uniformity causes a non-uniform temperature profile in the work-piece. A non-uniform current distribution can be caused by several electromagnetic phenomena, including (1) skin effect, (2) proximity effect, and (3) ring effect. These effects play an important role in understanding the induction heating phenomena. Before exploring the distribution of the magnetic field and eddy current it is imperative to understand the nature of electromagnetic properties of heated metals. [5]

I.3.1. Electromagnetic effects:

I.3.1.1. Skin effect:

As one may know from the basics of electricity, when a direct current flows through a conductor, the electrical current distribution within the conductor's cross section is uniform. However, when an AC flows through the same conductor, the current distribution is not uniform. The maximum value of the current density will always be located on the surface of the conductor with homogeneous electromagnetic physical properties; the current density will decrease from the surface of the conductor toward its center. This phenomenon of nonuniform current distribution within the conductor cross section is called the skin effect, which always occurs (though to a different degree) whenever there is AC flow. Therefore, the skin effect will be present in a workpiece located inside an induction coil. [1]

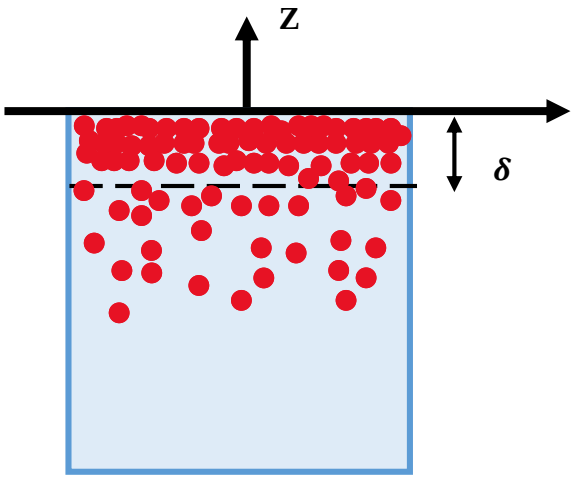

Fig.I.5. *Skin depth example.*

I.3.1.2. Proximity effect:

When discussing the skin effect in conductors or cables, it was assumed that a conductor stands alone and that there are no other current-carrying conductors in the surrounding area. In most practical applications, this is not the case. Most often, there are other conductors in proximity. These conductors have their own magnetic fields, which interact with nearby fields, affecting the current flow and power density distributions. [1]

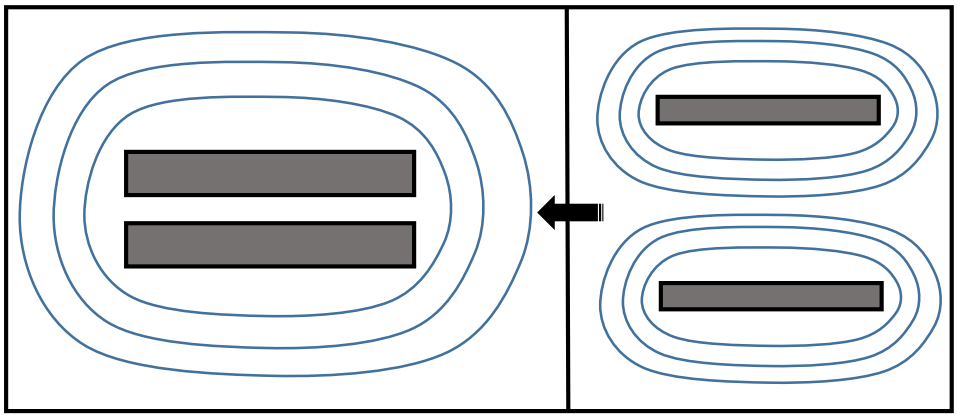

Fig.I.6. *Electromagnetic proximity effect.*

I.3.1.3. Ring effect:

Up to now, we have seen current density distribution in straight conductors. One such conductor, a rectangular bus bar, and its current distribution. If that current-carrying bar is bent to shape it into a ring, then its current will be redistributed. Magnetic flux lines will be concentrated inside the ring, increasing magnetic flux density there. Outside the ring, the magnetic flux lines will be disbursed.

As a result, most of the current will flow within the thin inside surface layer of the ring where there will be the shortest distance and the lowest impedance path. As one can see, this ring effect is also somewhat similar to the proximity effect because currents flowing on inside surfaces of the opposite sides of the ring's circumference are oriented in opposite directions (thus being attracted to each other). [1]

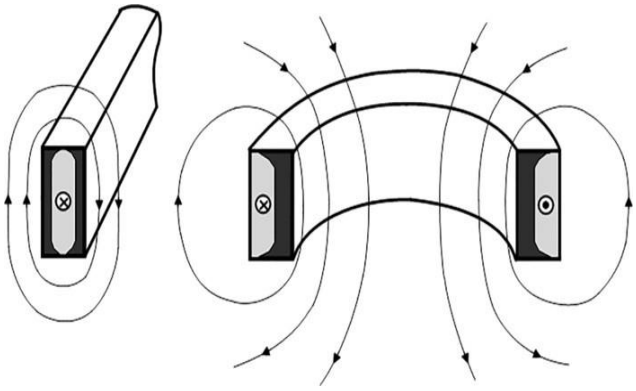

Fig.I.7. *Ring effect phenomena. [1]*

I.3.2. Estimation of the required power for induction heating:

Since the value of specific heat C_p represents the amount of the required heat energy to be absorbed by a unit mass of the work-piece to achieve a unit temperature increase, an average value of specific heat C_p can be effectively used for a ballpark estimate of the required work-piece power P_w to heat a given shape workpiece to an average temperature rise at the required production rate. The formula below can be used for this purpose,

$$\boldsymbol{P_w = m \times C_p \times \frac{T_f - T_i}{t}} \qquad \textbf{(I.29)}$$

Where m is the mass of the heated body, kg; $C_p$is the average value of specific heat, J/kg℃; T_i and T_f are average values of initial and final temperatures, ℃; and t is the required heat time, seconds.

For example, in order to heat a solid copper cylinder (*0.1m* diameter, *0.3m* long) from ambient temperature *20*℃ to a temperature *620*℃ in *120s*, the required power can be determined corresponding to the precedent formula.

In this case, the mass of the heated body can be calculated as;

$$m = \frac{\pi \times D^2}{4} \times L \times \rho = \frac{\pi \times 0{,}1^2}{4} \times 0.3 \times 8.91 \times 10^3 = 21kg$$

Where ρ is the density in kg/m^3 (for copper $\rho = 8.91 \times 10^3\ kg/m^3$), D is the diameter in m, and L is the billet length in m .

$c = 420\ J/kg$℃ Can be used as an average value of the specific heat of copper in the temperature range *20* to *620*℃. Therefore, applying the precedent equation, the required power will be;

$$P_w = m \times c \times \frac{T_f - T_i}{t} = 21 \times 420 \times \frac{620-20}{120} = 44100\ W = 44.1\ kW$$

I.3.3. Electromagnetic properties of metals:

Electromagnetic properties of materials are quite a broad expression that refers to a number of electromagnetic characteristics including magnetic permeability, electrical resistivity (electrical conductivity), saturation flux density, coercive force, hysteresis loss, initial permeability, permittivity, magnetic susceptibility, magnetic dipole moment, and many others. Recognizing the importance of all electromagnetic properties, we concentrate only on those properties that have the most pronounced effect on parameters of the induction heating systems.

I.3.3.1. Electrical resistivity (Electrical conductivity):

The ability of material to easily conduct electric current is specified by electrical conductivity σ. The reciprocal of the conductivity σ is electrical resistivity ρ_r. The units for ρ_r and σ are $\Omega.m$ and S/m, respectively. Both characteristics can be used in engineering practice, however, the majority of data books consist of data for electrical resistivity.

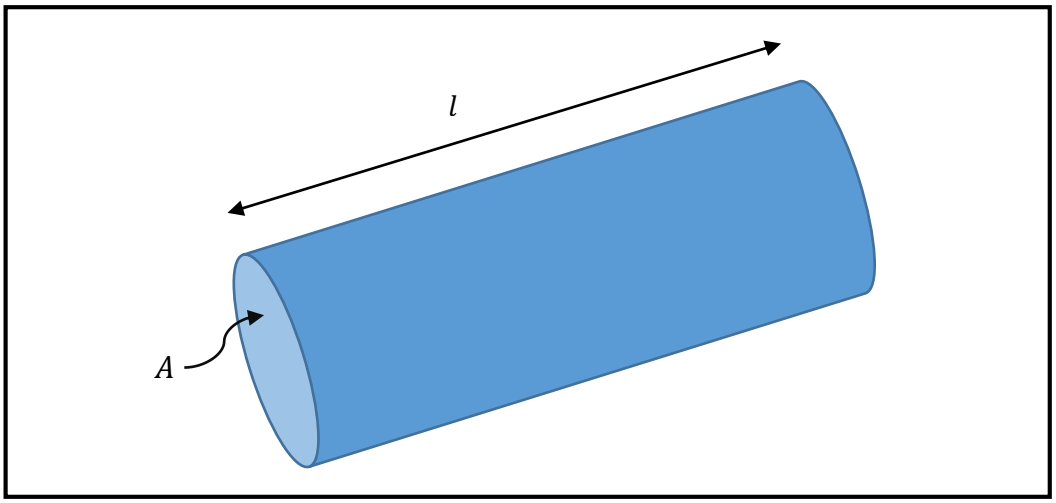

Fig.I.8. *A piece of resistive material with electrical contacts on both ends.*

In an ideal case, cross-section and physical composition of the examined material are uniform across the sample, and the electric field and current density are both parallel and constant everywhere. Many resistors and conductors do in fact have a uniform cross section with a uniform flow of electric current, and are made of a single material, so that this is a good model. See *Fig.I.8.* When this is the case, the electrical resistivity ρ_r can be calculated by:

$$\boldsymbol{\rho_r = R \times \frac{A}{l}} \qquad \textbf{(I.30)}$$

R: The electrical resistance of a uniform material.

A: The cross-sectional area of the material piece.

l: The length of the material piece.

And it is the inverse of conductivity.

$$\boldsymbol{\rho_r = \frac{1}{\sigma}} \qquad \textbf{(I.31)}$$

The above equation can be transposed to get Pouillet's law:

$$\boldsymbol{R = \rho_r \times \frac{l}{A}} \qquad \textbf{(I.32)}$$

Table.I.1. *Resistivity and Conductivity of materials at 20°C. [8]*

Material	Resistivity ρ_r [$\Omega.m$] at 20°C	Conductivity $\sigma[S/m]$ at 20 °C
Silver	1.59×10^{-8}	6.3×10^{7}
Copper	1.68×10^{-8}	5.96×10^{7}
Gold	2.44×10^{-8}	4.1×10^{7}
Tin	1.09×10^{-7}	9.17×10^{6}
Iron	1×10^{-7}	1×10^{7}
Air	1.3×10^{16} to 3.3×10^{16}	3×10^{-15} to 8×10^{-15}

I.3.3.2. Magnetic permeability and relative permittivity:

Relative magnetic permeability μ_r indicates the ability of a material to conduct the magnetic flux better than a vacuum or air. Relative permittivity ε indicates the ability of a material to conduct the electric field better than vacuum or air. Both relative magnetic permeability μ_r and relative permittivity ε are no dimensional parameters and have very similar meaning. Understanding the physics of these properties is important when designing heating systems.

Relative permeability denoted by the symbol μ_r, is the ratio of the permeability of a specific medium to the permeability of free space μ_0.

$$\mu_r = \frac{\mu}{\mu_0} \qquad \textbf{(I.33)}$$

Where μ_0 is the magnetic permeability of free space.

$$\mu_0 = 4\pi \times 10^{-7} \quad (\frac{H}{m})$$

Table.I.2. *Magnetic permeability for selected materials. [7]*

Materials	Permeability $\mu[H/m]$	Relative permeability $\frac{\mu}{\mu_0}$
Vacuum μ_0	$4\pi\times10^{-7}$ or 1.2566×10^{-6}	1
Air	1.2566×10^{-6}	1.00000037
Copper	-6.4×10^{-6} or -9.2×10^{-6}	0.999994
Tin	/	< 1
Aluminum	2.22×10^{-5}	1100°-1600°
Pure Iron (99.8%)	6.3×10^{-3}	1.000022

Relative magnetic permeability has a marked effect on all basic induction phenomena, including the skin effect, electromagnetic edge, and end effect, as well as proximity and ring effect, and also has a marked effect on coil calculation and computation of electromagnetic field distribution. Relative permittivity is not as widely used in induction heating, but it plays a major role in dielectric heating applications.

I.4. Eddy current:

I.4.1. Hysteresis and eddy current losses:

Induction heating takes place in an electrically conducting object, not necessarily magnetic steel, when the object is placed in a varying magnetic field. Induction heating is due to hysteresis and eddy current losses.

Hysteresis losses only occur in magnetic materials such as steel, nickel, and very few others. An old fashioned, but still useful, explanation of the hysteresis loss states that it is caused by friction between molecules when the material is magnetized first in one direction and then in the other. The molecules may be regarded as small magnets which turn around with each reversal of direction of the magnetic field. Work (energy) is required to turn them around. The energy converts into heat. The rate of expenditure of energy (power) increases with an increased rate of reversal (frequency). [1]

Eddy-current losses occur in any conducting material in a varying magnetic field. This causes heating, even if the materials do not have any of the magnetic properties usually associated with iron and steel. Eddy current are electric currents induced by transformer action in the material. As their name implies, they appear to flow around in swirls or eddies within a solid mass of material. Sometimes eddy currents flow in a portion of an electrical machine where we do not want any current flow at all. [1]. Heating due to eddy currents is simple I^2R heating the same as current flowing through a light bulb filament or an electric resistance heater. In the study of induction heating, we are very much interested in the behavior of eddy currents. One of the first things we note about them is that they follow the simple laws of electricity.

Eddy-current losses are much more important than hysteresis losses in induction heating. Note that induction heating is applied to nonmagnetic materials, where no hysteresis losses occur. For the heating of steel for hardening, forging, melting, or any other purposes which require temperature above the Curie temperature (about $1425°F$), we cannot depend upon hysteresis. Steel loses its magnetic properties above this temperature. Just when heat is needed most, hysteresis disappears. When steel is heated below the Curie point, the contribution of hysteresis is usually so small that it can be ignored. For all practical purpose, the I^2R of the eddy currents is the only way in which electrical energy can be turned into heat for induction heating purposes. [1]

I.4.2. Magnetic field around a current-carrying conductor:

We know from the study of electricity that current flowing through a conductor sets up a magnetic field around the conductor. The direction of the field depends upon the direction of the current and is given by the right-hand rule, if the conventional direction of current flow (Franklinian) is assumed.

If the current flow in the conductor reverses, the field around the conductor also reverses. Likewise, if the current is alternating, the field set up by the current alternates too. When the current is maximum, the field is maximum. If the conductor is bent into a long circular coil (a solenoid), the effects of the current flowing in the various turns add to each other, and the magnetic field is strengthened. By the right-hand rule for a current-carrying solenoid, the fingers represent the direction of current flow around the solenoid, and the thumb gives the direction of the magnetic field. [1]

I.5. Governing equations:

Electromagnetic induction is a physical phenomenon which among by the work of Emil Lenz and Michael Faraday on electromagnetic fields. It is a phenomenon producing electromotive forces in a conductive material when it is subjected to a variable electromagnetic field. In order to study this phenomenon, it is necessary to introduce Maxwell's equations.

Maxwell-Gauss *Eq. (I.34).* The density of electric charges is the source of the electric displacement field *D*. Here we will consider that the charges are distributed homogeneously in the materials.

$$\boldsymbol{\nabla \times D = 0} \qquad \textbf{(I.34)}$$

Maxwell-Thomson *Eq. (I.35),* also called conservation of magnetic flux. This equation translates the fact that the lines of magnetic induction *B* always loop back.

$$\boldsymbol{\nabla \times B = 0} \qquad \textbf{(I.35)}$$

Maxwell-Faraday *Eq. (I.36).* The temporal variation of the magnetic induction is linked to a spatial variation of the electric field *E*.

$$\boldsymbol{\nabla \times E = -\frac{\partial B}{\partial t}} \qquad \textbf{(I.36)}$$

Maxwell-Ampere *Eq. (I.37).* The spatial variation of the magnetic field *H* is related to the temporal variation of the electric displacement field as well as to the electric current density *J*.

$$\boldsymbol{\nabla \times H = J + \frac{\partial D}{\partial t}} \qquad \textbf{(I.37)}$$

We notice that equations *Eq. (I.36)* and *Eq. (I.37)* highlight a strong coupling between electric and magnetic phenomena.

The modified Navier-Stokes equations under the effect of magnetic field body force including induction and energy equation in vector forms are respectively

Navier-Stokes equation: $$\boldsymbol{\frac{\partial \vec{V}}{\partial t} + \vec{V}.\vec{\nabla}(\vec{V}) = -\frac{1}{\rho}\vec{\nabla}\,\vec{P} + \frac{1}{\rho}\overrightarrow{F_{em}} + \nu_f \nabla^2 \vec{V}} \qquad \textbf{(I.38)}$$

Continuity equation: $$\boldsymbol{\vec{\nabla}.\vec{V} = 0} \qquad \textbf{(I.39)}$$

Lorentz force: $$\boldsymbol{\overrightarrow{F_{em}} = \vec{J} \times \vec{B} = \underbrace{-\frac{1}{2\mu}\vec{\nabla}\,B^2}_{Magnetic\ pressure} + \underbrace{\frac{1}{\mu}(\vec{B}.\vec{\nabla})\,\vec{B}}_{Magnetic\ tension}} \qquad \textbf{(I.40)}$$

The flow of conducting fluid generates an induction magnetic field B_Z, satisfying:

Induction equation: $\frac{\partial \vec{B}}{\partial t} = \vec{\nabla} \times \left(\vec{V} \times \vec{B}\right) + \lambda \nabla^2 \vec{B}$ **(I.41)**

I.5.1. Induction equation:

It is very useful to consider the magnetic field B as the principal electromagnetic quantity. All the other quantities (E, J) can in fact be simply deduced from B using Maxwell's equations and Ohm's law as:

$$\vec{\nabla}.\vec{B} = 0 \quad \textbf{(I.42)}$$

Electromagnetic fields are described by Maxwell's equations:

$$\vec{\nabla} \times \vec{E} = -\frac{\partial \vec{B}}{\partial t} \quad \textbf{(I.43)}$$

$$\vec{\nabla} \times \vec{H} = \vec{j} + \frac{\partial \vec{D}}{\partial t} \quad \textbf{(I.44)}$$

The induction fields H and D are defined as,

$$\vec{\mathbf{H}} = \frac{\mathbf{1}}{\mu}\vec{\mathbf{B}} \quad \textbf{(I.45)}$$

$$\vec{\mathbf{D}} = \boldsymbol{\varepsilon}\vec{\mathbf{E}}$$

In general Ohm's law that defines the current density is given by:

$$\vec{j} = \sigma\vec{E}$$

With:

$\vec{j}$**:** Current density.

σ**:** Electrical conductivity.

$\vec{E}$**:** Electric field.

For fluid velocity field v in a magnetic field B,

$$\vec{j} = \sigma\left(\vec{E} + \vec{v} \times \vec{B}\right) \quad \textbf{(I.46)}$$

Of *Eq. (I.39)* we have:

$$\frac{\partial \vec{B}}{\partial t} = -\vec{\nabla} \times \vec{E} \quad \textbf{(I.47)}$$

We have:

$$\vec{E} = \frac{\vec{J}}{\sigma} - \vec{V} \times \vec{B} \quad \textbf{(I.48)}$$

Take the curl:

$$\vec{\nabla} \times \vec{E} = \vec{\nabla} \times \left[\frac{\vec{j}}{\sigma} - \vec{V} \times \vec{B}\right] \quad \textbf{(I.49)}$$

Inserting *Eq. (I.49)* into *Eq. (I.47)* we get:

$$\frac{\partial \vec{B}}{\partial t} = -\vec{\nabla} \times \left[\frac{\vec{j}}{\sigma} - \vec{V} \times \vec{B}\right] \quad \textbf{(I.50)}$$

$$\frac{\partial \vec{B}}{\partial t} = -\vec{\nabla} \times \left(\frac{\vec{j}}{\sigma}\right) + \vec{\nabla} \times \left(\vec{V} \times \vec{B}\right) \quad \textbf{(I.51)}$$

If the displacement current neglected customarily, we rewrite *Eq. (I.44)* as:

$$\vec{\nabla} \times \vec{H} = \vec{j} \quad \textbf{(I.52)}$$

With using *Eq. (I.45)* we get:

$$\frac{1}{\mu}\left(\vec{\nabla} \times \vec{B}\right) = \vec{j} \quad \textbf{(I.53)}$$

If we substitute *Eq. (I.53)* into *Eq. (I.51)* we get:

$$\frac{\partial \vec{B}}{\partial t} = -\vec{\nabla} \times \left(\frac{1}{\mu\sigma}\left(\vec{\nabla} \times \vec{B}\right)\right) + \vec{\nabla} \times \left(\vec{V} \times \vec{B}\right) \quad \textbf{(I.54)}$$

Could be written as:

$$\frac{\partial \vec{B}}{\partial t} = -\frac{1}{\mu\sigma}\vec{\nabla} \times \left(\vec{\nabla} \times \vec{B}\right) + \vec{\nabla} \times \left(\vec{V} \times \vec{B}\right) \quad \textbf{(I.55)}$$

$$\vec{V} = \left(0, 0, w(x, y)\right) \qquad \vec{B} = \left(0, B_0, B_Z(x, y)\right)$$

Here if we use the very well-known property:

$$a \times (b \times c) = b(a.c) - c(a.b)$$

Rewrite *Eq. (I.55),*

$$\frac{\partial \vec{B}}{\partial t} = -\frac{1}{\mu\sigma}\left[\vec{\nabla}\left(\vec{\nabla}.\vec{B}\right) - \vec{B}\left(\vec{\nabla}.\vec{\nabla}\right)\right] + \vec{V}\left(\vec{\nabla}.\vec{B}\right) - \vec{B}\left(\vec{\nabla}.\vec{V}\right) \quad \textbf{(I.56)}$$

With using *Eq. (I.42),*

$$\frac{\partial \vec{B}}{\partial t} = -\frac{1}{\mu\sigma}\nabla^2\vec{B} + \vec{V}\left(\vec{\nabla}.\vec{B}\right) - \vec{B}\left(\vec{\nabla}.\vec{V}\right) \quad \textbf{(I.57)}$$

From *Eq. (I.45),* we have:

$$\vec{B} = \mu\vec{H} \quad \textbf{(I.58)}$$

In steady-state condition and with using *Eq. (I.58),* we get:

$$\frac{1}{\mu\sigma}\mu\nabla^2\vec{H} - \mu\vec{V}\left(\vec{\nabla}.\vec{H}\right) + \mu\vec{H}\left(\vec{\nabla}.\vec{V}\right) = 0 \quad \textbf{(I.59)}$$

Multiply by $\boldsymbol{\sigma}$,

$$\boldsymbol{\nabla}^{\mathbf{2}}\overrightarrow{\boldsymbol{H}} + \boldsymbol{\sigma}\mu\left[\left(\overrightarrow{\boldsymbol{H}}.\overrightarrow{\boldsymbol{\nabla}}\right)\overrightarrow{\boldsymbol{V}} - \left(\overrightarrow{\boldsymbol{V}}.\overrightarrow{\boldsymbol{\nabla}}\right)\overrightarrow{\boldsymbol{H}}\right] = \mathbf{0} \quad \textbf{(I.60)}$$

Eq. (I.60) is the induction equation derived from Ohm's law and Maxwell's equations.

Where $\vec{J}$ is the current density due to the magnetic field, $\vec{E}$ is the electric field intensity, ρ is density of the fluid, σ is the electrical conductivity, $\mu = \rho\nu$ and is the coefficient of viscosity, ν is the kinematic viscosity, μ_e is magnetic permeability and is the magnetic diffusivity.

I.5.2. Energy equation:

$$\boldsymbol{\rho C_P}\left[\frac{\partial\vec{T}}{\partial t} + \left(\vec{V}.\boldsymbol{\nabla}\right)\vec{T}\right] = \boldsymbol{\nabla}\left(\boldsymbol{\lambda}\boldsymbol{\nabla}\vec{T}\right) + \overrightarrow{\boldsymbol{\phi}} + \overrightarrow{\boldsymbol{P_e}} \quad \textbf{(I.61)}$$

Where T is the volume-averaged equilibrium temperature for both the solid and the porous medium, C_P the specific heat of the fluid, k the effective thermal conductivity of the porous medium, and ϕ is the contribution due to viscous dissipation.

$$\boldsymbol{V = RI} \quad \textbf{(I.62)}$$

With:

V: Voltage in volts.

I: Current in amps.

R: Resistance in ohms.

$$\boldsymbol{P = VI \longrightarrow P = RI^2} \quad \textbf{(I.63)}$$

Where:

P: Mechanical power.

$$\boldsymbol{R_e = \frac{L}{\sigma S} \longrightarrow P = \frac{L}{\sigma S} I^2} \quad \textbf{(I.64)}$$

Were, R_e: The electrical resistance.

$$\boldsymbol{P = \frac{LS}{\sigma S^2} I^2} \quad \textbf{(I.65)}$$

$$\boldsymbol{P = \frac{V}{\sigma S^2} I^2} \qquad \text{With} \qquad \boldsymbol{V = LS} \quad \textbf{(I.66)}$$

$$\boldsymbol{\frac{P}{V} = \frac{J^2}{\sigma}} \qquad \text{With} \qquad \boldsymbol{J = \frac{I}{S}} \quad \textbf{(I.67)}$$

The viscous dissipation contribution is expressed as:

$$\boldsymbol{\phi = \mu_{eff}\left(\frac{du}{dy}\right)^2} \quad \textbf{(I.68)}$$

$$\boldsymbol{\rho C_P (V.\nabla) T = \lambda \nabla^2 T + \phi + \frac{J^2}{\sigma}} \quad \textbf{(I.69)}$$

I.6. Induction melting:

In the production of metal, it is necessary to raise the temperature of the metal or to the melting point and often to hold it at temperature to allow some type of metallurgical treatment. Electric furnaces used in the melting process are induction, arc, or resistance furnaces. The typical induction melting furnaces in use are the channel type and the crucible type that allow one to melt irons, steels, aluminum, copper, tin, zinc, nickel, and other metals and alloys.[6]

A major advantage that is inherent with induction melting is inductive stirring. In an induction furnace, the metal charge material is melted or heated by current generated by an electromagnetic field. When the metal becomes molten, this field also causes the bath to move. This is called inductive stirring. This constant motion naturally mixes the bath producing a more homogeneous mix and assists with alloying. The amount of stirring is determined by the size of the furnace, the power put into the metal, the frequency of the electromagnetic field and the type/amount of metal in the furnace. The amount of inductive stirring in any given furnace can be manipulated for special applications if required. [6]

Because induction heating is accomplished using a magnetic field, the work piece (or load) can be physically isolated from the induction coil by refractory or some other non-conducting medium. The magnetic field will pass through this material to induce a voltage in the load contained within. This means that the load or work piece can be heated under vacuum or in a carefully controlled atmosphere. This enables processing of reactive metals (Ti, Al), specialty alloys, silicon, graphite, and other sensitive conductive materials.

Bibliography

[1] Chester A, Tudbury, Basics of induction heating, John F, Rider, 1960.

[2] Heng Liu, FME Simulations of induction hardening process, Master thesis, 2013.

[3]https://www.umsl.edu/physics/Lab%20Connection/Electricity%20and%20Magnetism%20Lab/12-lab6.html.

[4] Sari Ibrahim, Study of the effect of forced convection by electromagnetic stirring on the phase change process: Application on the metallic alloy solidification, doctoral thesis 2021.

[5] Zdenek Dostàl, Optimal control of induction heating processes, CRC Press, 2006.

[6] Valery Rudnev, Don Loveless, Raymond L. Cook, Handbook of Induction Heating, Second Edition, CRC Press;Cook, Raymond L., CRC Pr I Llc, Loveless, Don, Rudnev, Valery, 2017.

[7] https://en.wikipedia.org/wiki/Permeability_ (electromagnetism).

[8] https://www.thoughtco.com/table-of-electrical-resistivity-conductivity-608499.

Chapter two:

Phase change

II. Phase change:

II.1. Phase change phenomena:

II.1.1. Phase:

Phase, in thermodynamics, chemically and physically uniform or homogeneous quantity of matter that can be separated mechanically from a nonhomogeneous mixture and that may consist of a single substance or a mixture of substances. The three fundamental phases of matter are solid, liquid, and gas (vapor), but others are considered to exist, including crystalline, colloid, glassy, amorphous, and plasma phases. When a phase in one form is altered to another form, a phase change is said to have occurred. *Fig.II.1*

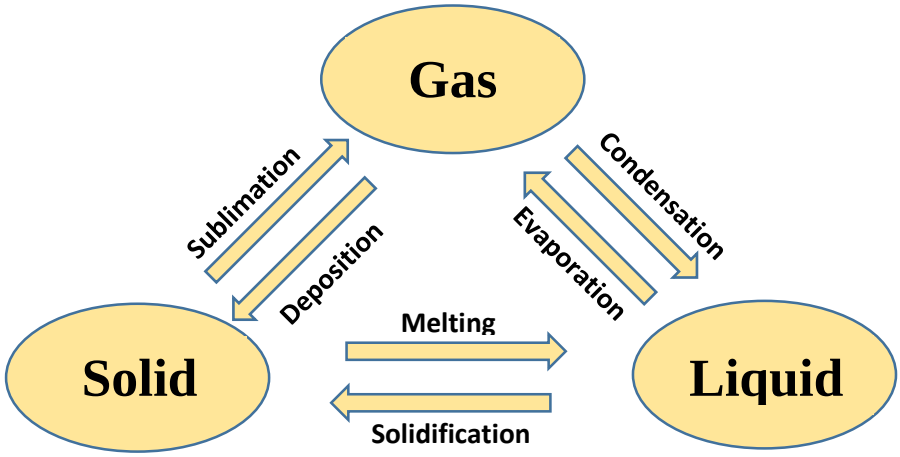

Fig.II.1. *Phase change of matter.*

II.1.2. Phase diagram:

Heating a metal or alloy to the melting temperature causes melting. The transition from the solid phase to the liquid phase is called a phase change (Melting).

Binary phase diagrams are the simplest diagrams to establish. The curves of the phase diagram determine the limits of the domains in which phases can exist, as well as the composition and proportions of these different phases.

When a pure metal is fused, under constant pressure (atmospheric pressure for example), the phase change always takes place at a fixed temperature which presents the melting point. At the melting point, the two liquid and solid phases coexist.

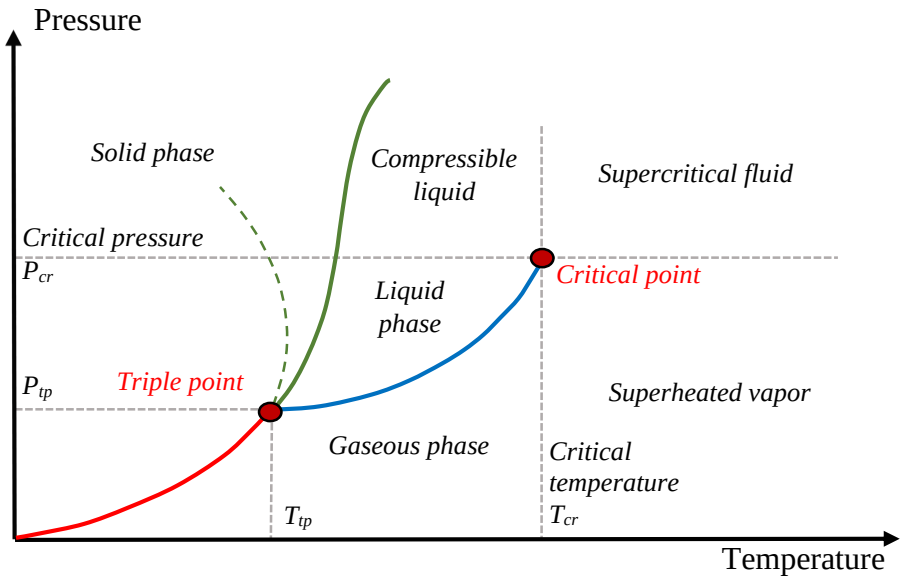

Fig.II.2. *phase diagram.*

II.1.3. Phase rule:

The classification and limitations of phase changes are described by the phase rule, as proposed by the American chemist J. Willard Gibbs in *1876* and based on a rigorous thermodynamic relationship. The phase rule is commonly given in the form $P + F = C + 2$. The term P refers to the number of phases that are present within the system, and C is the minimum number of independent chemical components that are necessary to describe the composition of all phases within the system. The term F, called the variance, or degrees of freedom, describes the minimum number of variables that must be fixed in order to define a particular condition of the system.

II.1.4. Overview of the phase change phenomena:

Several mechanisms are at work when a solid melts or a liquid solidifies, such a change of phase involved heat and often mass transfer, possible super cooling, absorption or release of latent heat, changes in thermos-physical proprieties, surface effects, etc.

It is important to note that although the focus of our discussions is melting. The principles, ideas and many of the results apply as well to other first-order phase transitions, vapor condensation and evaporation (gas-liquid transition), sublimation (gas-solid transition), or even certain magnetization phenomena.

Both solid and liquid phases are characterized by the presence of cohesive forces keeping atoms in close proximity. In a solid the molecules vibrate around fixed equilibrium positions, while in a liquid they may skip between these positions. The macroscopic manifestation of this vibrational energy is what we call heat or thermal energy, the measure of which is temperature.

Clearly atoms in the liquid phase are more energetic (hotter) than those in the solid phase, all other things being equal. Thus, before a solid can melt it must acquire a certain amount of energy to overcome the binding forces that maintain its solid structure. This energy is referred to as the latent heat L (heat of fusion) of the material, latent heat of fusion for some metals are indicated in *Table.II.1*, and represents the difference in thermal energy (enthalpy) levels between liquid and solid states, all other things being equal. Of course, solidification of liquid requires the removal of this latent heat and the structuring of atoms into more stable positions. In either case there is a major re-arrangement of the entropy of the material, a characteristic of phase transitions. [9]

Table.II.1. *Latent heat of fusion of common metals. [15]*

Metals	**Latent heat of fusion**	
	[kJ/mol]	**[kJ/kg]**
Aluminum (Al)	**10.7**	**396**
Copper (Cu)	**13.1**	**206**
Gold (Au)	**12.5**	**63**
Tin (Sn)	**7**	**59**
Mercury (Hg)	**2.29**	**11.4**
Pure (Fe)	**13.8**	**247**

These are three possible modes of heat transferring a material; conduction, convection and radiation. Conduction is the transfer of kinetic energy between atoms by any of a number of ways, including collision of neighboring atoms and the movement of electrons; there is no flow or mass transfer of the material. This is how heat is transferred in an opaque solid. In a liquid heat can also be transferred by the flow of particles, i.e., by convection. Radiation is the only mode of energy transfer that can occur in a vacuum (it requires no participating medium). Thermal radiation, emitted by the surface of a heated solid, is radiation of wave-length roughly in the range *0.1* to *10* microns meter (μm).

The transition from one phase to other, that is, the absorption or release of the latent heat, occurs at some temperature at which the stability of one phase breaks down in favor of the other according to the available energy. This phase change, or melt temperature *Tm* depends on pressure. Under fixed pressure, T_m may be a particular fixed value characteristic of the material (for example, *0*℃ for pure water freezing under atmospheric pressure), or a function of other thermodynamic variables (for example, of glycol concentration in an anti-freeze mixture).

II.1.5. Interface of phase change (Melting):

The phase-transition region where solid and liquid coexist is called the interface. Its thickness may vary from a few angstroms to a few centimeters, and its microstructure may be very complex, depending on several factors (the material itself, the rate of cooling, the temperature

gradient in the liquid, surface tension, etc.). For most pure materials solidifying under ordinary freezing conditions at a fixed T_m the interface appears (locally) planar and negligible thickness. Thus, it may be thought of as a "sharp front", a surface separating solid from liquid at temperature T_m. In other cases, typically resulting from super-cooling, the phase-transition region may have apparent thickness and is referred to as a ‘’mushy zone’’, its microstructure may now appear to be dendritic or columnar (shown in *Fig.II.3*). The local freezing temperature at a curved solid surface facing the liquid becomes depressed by an amount depending on the solid-liquid surface tension and the local curvature. This so-called Gibbs-Thomson effect is small for the overall freezing process, but crucial for the resulting microstructure of the interface. [9]

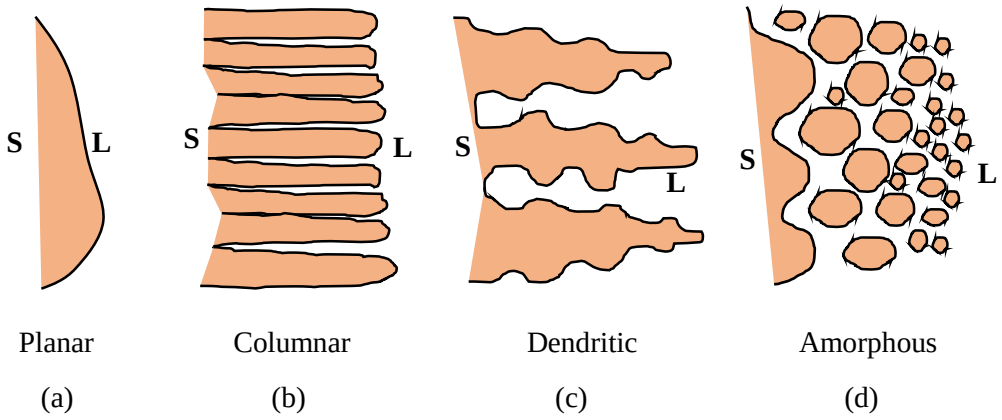

Fig.II.3. *Common interfacial morphology.*

II.1.6. Latent heat:

We can be established a relationship between latent heat and melting temperature using thermodynamic principles. The melting temperature is defined as the temperature at which the free energies of the two phases are equal. This therefore implies that at the melting temperature, the liquid and the solid have the same energy available to perform external work. The equilibrium between the solid and liquid phases can be expressed by *Eq. (II.1),* [10]

$$\boldsymbol{G_L = G_s} \qquad \textbf{(II.1)}$$

G: Gibbs free energy of the liquid and the solid.

$$\boldsymbol{G = H + TS} \qquad \textbf{(II.2)}$$

From *Eq. (II.1)* and *Eq. (II.2)* we get:

$$\boldsymbol{H_L + T_E S_L = H_S + T_E S_S} \qquad \textbf{(II.3)}$$

T_E: The equilibrium temperature.

$$\boldsymbol{H_L - H_S = L} \quad \textbf{(II.4)}$$

$$\boldsymbol{L = T_E \Delta S} \quad \textbf{(II.5)}$$

$$\boldsymbol{\Delta S = \frac{L}{T_E}} \quad \textbf{(II.6)}$$

The latent heat of melting L must be extracted from the system. For the fusion to take place, it is necessary that $\Delta G > 0$, which means, $G_S - G_L > 0$

The melting condition is: $\Delta G_V > 0 \Leftrightarrow T_m - T < 0 \Leftrightarrow T > T_m$

II.1.7. Melting of a pure substance:

The liquid-solid phase change of a pure substance or an alloy gives rise to the appearance of a transition zone between the two phases. In the microscopic scale, this zone is an interface of discontinuity, but it can become so geometrically complex that it appears on the macroscopic scale as diffuse and continuous transition zone.

The phase change results two main characteristics:

- A temperature can define in the interface of the two phases, it determined by the thermodynamic equilibrium relations.
- The phase change causes an absorption of heat in fusion (release of heat in solidification) proportional to the rate of phase change and localized at the interface.

In the pure substance case, the temperature T of the phase change interface is a physical constant. It can admit small variations depending on the importance of the f curved of the interface and the interfacial tension. [10]

$$\boldsymbol{T_f = T_{f0} - \gamma k} \quad \textbf{(II.7)}$$

$\boldsymbol{\gamma}$ And $\boldsymbol{k}$ defining the interfacial tension and the local curvature of the interface.

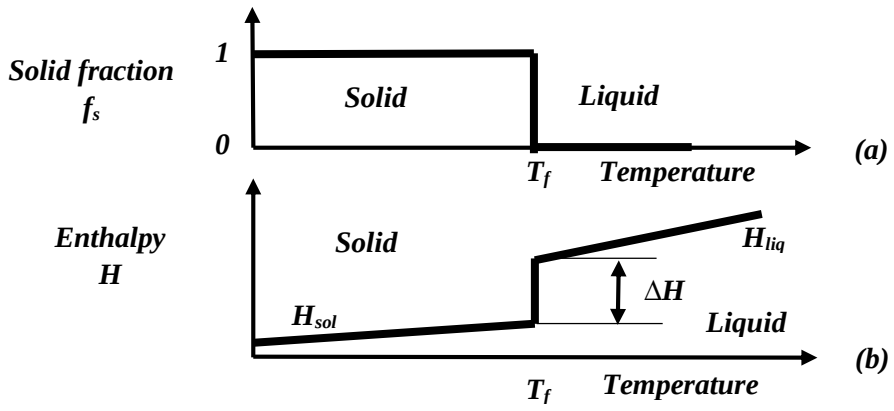

Fig.II.4. *Evolution of the solid fraction $f_S(a)$ and the enthalpy $H(b)$ when crossing the solidification front in the case where there is no solidification interval.*

To describe the phenomenon, it is convenient to use the specific enthalpy of the material *H (J/Kg)*, which is generally linear function of the temperature *T*,

$$\begin{cases} \boldsymbol{H_l = C_{Pl}T_l + H_{l0}} & \textit{for the liquid} \\ \boldsymbol{H_S = C_{PS}T_s + H_{S0}} & \textit{for the solid} \end{cases} \qquad \textbf{(II.8)}$$

$T_S, T_l, C_{PS}, C_{Pl},$ are the temperature and specific heat of solid and liquid.

$$\boldsymbol{\Delta H(T_f) = H_l(T_f) - H_S(T_f) = (C_{Pl} - C_{Ps})T_f + (H_{l0} - H_{S0})} \qquad \textbf{(II.9)}$$

Which represent the latent heat of phase change, the augmentation of the enthalpy on function of the temperature is illustrated in *Fig. (II.4).*

II.1.8. Melting of an alloy:

If the body contains impurities or other elements (alloys for solids, solutions for liquids), melting is a much more complex phase change. The phase change occurs in a $T_l - T_s$ temperature interval, called the melting interval. The quantities T_l and T_s are called the liquidus and solidus temperature respectively. Geometrically, there is a transition zone, the mushy zone, where the temperature is between T_l and T_s and which consists of a porous solid containing liquid occupying the interstices as shown in *Fig.II.5*. During melting, the percentage of solid volume, the solid fraction f_s is decreasing. [10]

From a macroscopic point of view, the problem can be treated due to the use of macroscopic variables such as the liquid or solid fractions and the enthalpy of the mixture (liquid + solid) defined as follows:

$$\boldsymbol{\bar{\rho} H = \rho_s f_s H_s + \rho_l f_l H_l} \qquad \textbf{(II.10)}$$

With: $\begin{cases} \boldsymbol{f_s + f_l = 1} \\ \boldsymbol{\bar{\rho} = \rho_s f_s + \rho_l f_l} \end{cases}$

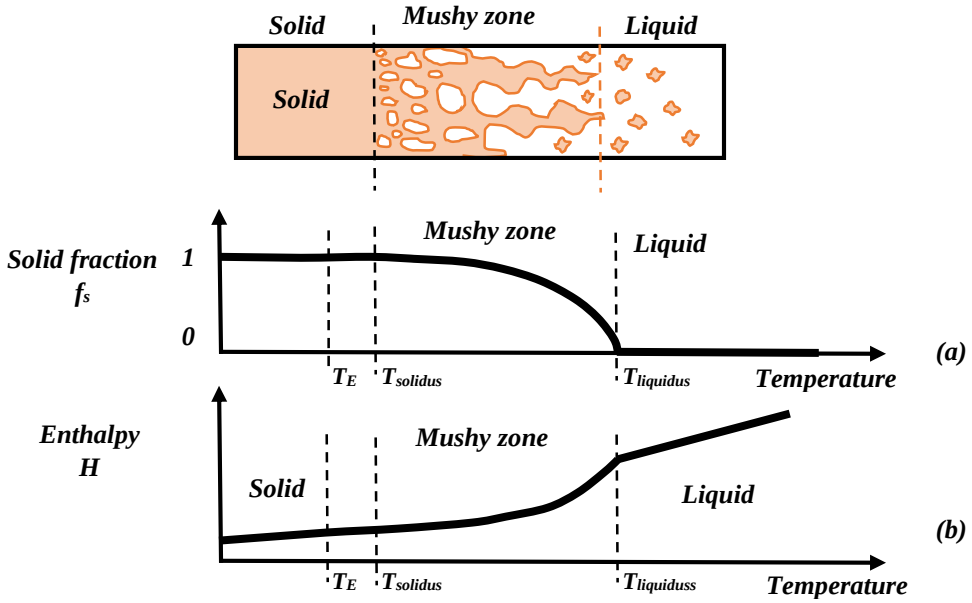

Fig.II.5. *(a) Evolution of the solid fraction f_s and (b) Evolution of the enthalpy, during the fusion transition of an alloy.*

II.2. Melting:

II.2.1. Melting (solid-liquid):

Melting, change of a solid into a liquid when heat is applied. In a pure crystalline solid, this process occurs at a fixed temperature called the melting point; an impure solid generally melts over a range of temperatures below the melting point of the principal component. Amorphous (non-crystalline) substances such as glass or pitch melt by gradually decreasing in viscosity as temperature is raised, with no sharp transition from solid to liquid.

The structure of a liquid is always less ordered than that of the crystalline solid and, therefore, the liquid commonly occupies a larger volume. The behavior of ice, which floats on water, and of a few other substances are notable exceptions to the usual decrease in density upon melting.

Melting of a given mass of a solid requires the addition of a characteristic amount of heat, the heat of fusion. In the reverse process, the freezing of the liquid to form the solid, the same quantity of heat must be removed. The heat of fusion of ice, the heat required to melt one gram, is about *80* calories; this amount of heat would raise the temperature of a gram of liquid water from the freezing point.

II.2.2. Melting point:

Melting point, temperature at which the solid and liquid forms of a pure substance can exist in equilibrium. As heat is applied to a solid, its temperature will increase until the melting point is reached, *Table.II.2*. More heat then will convert the solid into a liquid with no temperature change. When all the solid has melted, additional heat will raise the temperature of the liquid. The melting temperature of crystalline solids is a characteristic figure and is used to identify pure compounds and elements. Most mixtures and amorphous solids melt over a range of temperatures.

The melting temperature of a solid is generally considered to be the same as the freezing point of the corresponding liquid; because a liquid may freeze in different crystal systems and because impurities lower the freezing point, however, the actual freezing point may not be the same as the melting point. Thus, for characterizing a substance, the melting point is preferred.

Table.II.2. *Melting points of common metals. [11]*

Metals	Melting point °C
Aluminum (Al)	660°
Copper (Cu)	1080°
Gold (Au)	1053°
Tin (Sn)	232°
Steel	1100°-1600°
Pure Iron (Fe)	1535°

II.2.3. Thermodynamics:

For a solid to melt, heat is required to raise its temperature to the melting point. However, further heat needs to be supplied for the melting to take place, this is called the heat of fusion, and is an example of latent heat.

From a thermodynamics point of view, at the melting point the change in Gibbs free energy *(ΔG)* of the material is zero, but the enthalpy *(H)* and the entropy *(S)* of the material are increasing *(ΔH, ΔS > 0)*. Melting phenomenon happens when the Gibbs free energy of the liquid becomes lower than the solid for that material. At various pressures this happens at a specific temperature. It can also be shown that:

$$\mathbf{\Delta S} = \frac{\mathbf{\Delta H}}{\boldsymbol{T}} \qquad \textbf{(II.11)}$$

Here T, ΔS and ΔH are respectively the temperature at the melting point, change of entropy of melting and the change of enthalpy of melting ΔH Enthalpy change in J,

ΔS: Variation of entropy in J/K.

m: mass in kg.

T: Temperature in K.

The melting point is sensitive to extremely large changes in pressure, but generally this sensitivity is orders of magnitude less than that for the boiling point, because the solid-liquid transition represents only a small change in volume. If, as observed in most cases, a substance is denser in the solid than in the liquid state, the melting point will increase with increases in pressure. Otherwise, the reverse behavior occurs.

Melting points are often used to characterize organic and inorganic compounds and to ascertain their purity. The melting point of a pure substance is always higher and has a smaller range than the melting point of an impure substance or, more generally, of mixtures. The higher the quantity of other components, the lower the melting point and the broader will be the melting point range, often referred to as the "pasty range". The temperature at which melting begins for a mixture is known as the "solidus" while the temperature where melting is complete is called the "liquidus". Eutectics are special types of mixtures that behave like single phases. They melt sharply at a constant temperature to form a liquid of the same composition. Alternatively, on cooling a liquid with the eutectic composition will solidify as uniformly dispersed, small (fine-grained) mixed crystals with the same composition. [11]

II.3. Mathematical model of melting:

In general, numerical simulations commonly used for phase change problems are classified into two different approaches: the fixed-grid and the transformed-grid methods, the fixed-grid method used a single set of conservation equation and boundary conditions for the whole domain comprising the solid and liquid phases, while the transformed-grid method employs the governing equations based on the classical Stefan formulation. The interface conditions, therefore, are accounted for differently according to the method incorporated in solving the phase change

problem. In the transformed-grid method, they are easily imposed because the interface is explicitly solved. However, in the fixed-grid method, the interface conditions are described as suitable source terms in the governing equations. A nodal latent heat value is assigned to each computational cell according to its temperature or enthalpy. Upon phase changing, the latent heat absorption, or evolution, is reflected as a source, or sink term in the energy equation. [12]

When melting a certain metal in his liquid phase bath, where the bath has a temperature of T_L, the initial temperature of the solid in uniform at T_0, and after immersion, the interface acquires the melting temperature of T_m. The traditionally used melting equations written in one dimension are,

$$\boldsymbol{h(T_L - T_m) = \rho L_f - \lambda_s \frac{\partial T}{\partial x}\Big|_{int}} \quad \textbf{(II.12)}$$

And

$$\boldsymbol{\frac{\partial}{\partial x}\left(\lambda_s \frac{\partial (C_p T)}{\partial (t)}\right)} \quad \textbf{(II.13)}$$

Where k_s is the thermal conductivity, defined only in the solid metal, ρ is the mass density in the solid metal, C_p is the specific heat in the solid metal, h is the heat-transfer coefficient between the liquid and solid, L_f is latent heat of melting and v in the moving velocity of the interface (melting rate). *Eq. (II.12)* represents the heat balance at the interface, and *Eq. (II.13)* describe the heat conduction in the solid metal. [12]

II.3.1. Enthalpy-porosity method:

The fixed-grid method requires the velocity suppression because as a liquid region turns solid, the zero-velocity condition should be satisfied. The velocity suppression can be accomplished by a large value of viscosity for the solid phase or by a suitable source term in the momentum equation to model the two-phase domain as a porous medium. The fixed-grid method combined with the porous medium method is usually referred to as the enthalpy-porosity method. The enthalpy-porosity method example is taken from references [13], [12].

II.3.1.1. Heating stage:

To simulate the melting process in a circular scrap melter a simplified one-dimensional heat transfer model is built using enthalpy formulation and porosity to describe scrap geometry. Scrap metal is filled in a cylindrical furnace with height H and diameter D.

The burner is located at the top of the furnace. The peripheral surface and the bottom are adiabatic. [12]

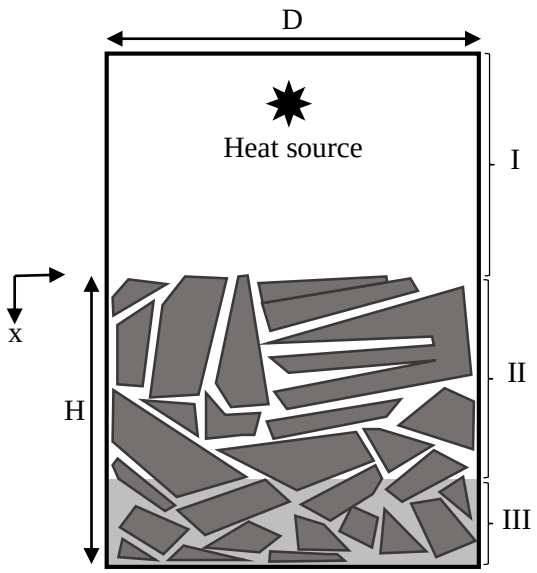

Fig.II.6. *Schematic representation of the three regions of a melting furnace.*

During the heating stage, there is no liquid metal present in the furnace. The third region does not exist. Only the second region, the solid-gas phase, is to be considered. As it is impossible to solve the fluid flow and heat transfer within each individual gap between the scraps, the lump of scrap metal is treated as a pseudo-porous medium. As a result, the heat transfer mechanisms consist of heat conduction from contacts between the scraps is accounted for by invoking a porosity factor. Heat transfer by gas flow and radiation from the flame is included into a source term.

With the foregoing considerations, the governing equation for the melting of scrap metal may be stated as follows,

$$\boldsymbol{\rho C_p \frac{\partial T}{\partial t} = \frac{\partial}{\partial x}\left(\lambda \frac{\partial T}{\partial x}\right) + q} \qquad \textbf{(II.14)}$$

Where, q is the heat source density and K is the bulk thermal conductivity and it is function of the porosity,

$$\boldsymbol{K = \lambda_s(1 - \delta_i)} \qquad \textbf{(II.15)}$$

Where, k_s is the conductivity of the solid and δ_i is the porosity, subscript i denotes gas or molten liquid by g or l respectively, ρ and C_p are calculated in similar way as K, ρ is in reality ρ_{eff},

$$\boldsymbol{\rho_{eff} = \rho(1 - \delta_i)} \qquad \textbf{(II.16)}$$

$\delta_g = 1$, mean that the space in the porosity is filled with gas only, and $\delta_g = 0$ means that the space is filled with solid. The same is denoted in liquid, $\delta_g = 1$ space filled with liquid and $\delta_g = 0$ for a space filed with solid.

Fig.II.6, appears when the melting starts. The convective heat transfer from the molten liquid metal is taken into account by this new source term,

$$\boldsymbol{q_x h_l A_{eff}(T_b - T)} \quad \textbf{(II.17)}$$

h_l Is convective heat transfer coefficient of the liquid metal, A_{eff} is the effective area and T_b is bulk temperature of the liquid metal.

When the whole scrap metal is immersed into the molten liquid *Fig.II.7,* the second region disappears, and the last stage begins. The first region is the same as in the previous stage. The second region is a single phase (molten liquid), and the third region is the solid-liquid phase. In the liquid metal region, the bulk thermal conductivity in *Eq.II.14* becomes $K = \boldsymbol{\lambda_l}$. In the solid liquid region, the governing equation remains unchanged, except for the bulk thermal conductivity, which becomes $K = \boldsymbol{\lambda_s}(1 - \delta_i)$.

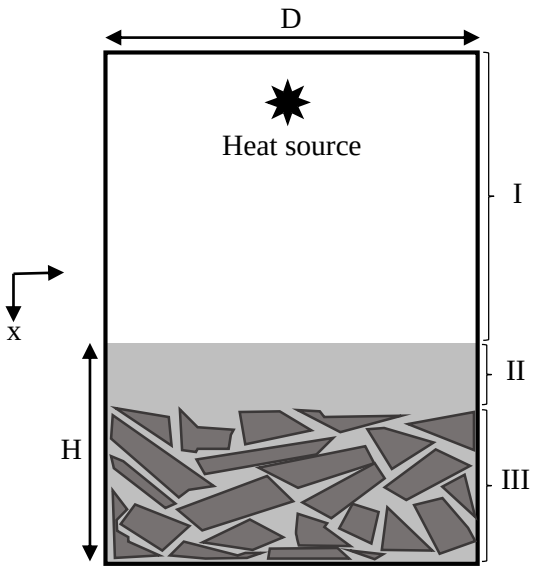

Fig.II.7. *when the whole scrap metal is immerged into the molten liquid, three new regions of a melting furnace occur.*

II.3.1.2. Enthalpy method:

Taking advantage of the axisymmetric geometry of the furnace and heating from the top, the phase change problem may be formulated in terms of a one-dimensional time-dependent model. An enthalpy-based method is retained and leads to the following energy equation for the total enthalpy H,

$$\frac{\partial \boldsymbol{H}}{\partial \boldsymbol{t}} = \boldsymbol{\nabla(\lambda \nabla T) + q} \quad \textbf{(II.18)}$$

The total enthalpy is further split into sensible enthalpy and latent heat components, i.e.

$$\boldsymbol{H = h + \rho f_l L} \quad \textbf{(II.19)}$$

L Is latent heat of fusion and h is sensible enthalpy, defined as,

$$\boldsymbol{h(T) = \int_{T_m}^{T} \rho C_p dT} \quad \textbf{(II.20)}$$

Where T_m is the melting temperature. The discrete form of the enthalpy-temperature relationship is,

$$\begin{cases} \boldsymbol{T = T_m + \frac{H - \rho L}{\rho C_p}} & \boldsymbol{H \geq \rho L} \quad (\boldsymbol{liquid\ phase}) \\ \boldsymbol{T = T_m} & \boldsymbol{0 \leq H \leq \rho L} \quad (\boldsymbol{mushy\ phase}) \\ \boldsymbol{T = T_m + \frac{H}{\rho C_p}} & \boldsymbol{H \leq 0} \quad (\boldsymbol{solid\ phase}) \end{cases} \quad \textbf{(II.21)}$$

The local liquid fraction f_l *Eq.II.19,* is defined as,

$$\begin{cases} \boldsymbol{f_1 = 1} & \boldsymbol{T > T_m} \\ \boldsymbol{f_2 = 0} & \boldsymbol{T < T_m} \end{cases} \quad \textbf{(II.22)}$$

Substitution of *Eq.II.19* and *Eq.II.20* into *Eq.II.18* yields,

$$\boldsymbol{\rho C_p \frac{\partial T}{\partial t} = \frac{\partial}{\partial x}\left(\lambda \frac{\partial T}{\partial x}\right) - \rho L \frac{\partial f_l}{\partial t} + q} \quad \textbf{(II.23)}$$

The potential advantage of this formulation is that the energy equation is cast into a standard form and the problems associated with the phase change are isolated in a source term (second term in *Eq. (II.23)*). q Is represents a heat source, the heat source follows the relation, [12]

Here in our case, when we melt the conductor material by Joule effect generated by eddy current which induced by a high frequency, the q is the volume heat which represents this phenomenon as detailed in the first chapter and expressed by *Eq. (II.24)* formulation.

$$\boldsymbol{q = \frac{j^2}{\sigma}} \quad \textbf{(II.24)}$$

We can rewrite *Eq. (II.23)* as:

$$\boldsymbol{\rho C_p \frac{\partial T}{\partial t} = \frac{\partial}{\partial x}\left(\lambda \frac{\partial T}{\partial x}\right) - \rho L \frac{\partial f_l}{\partial t} + \frac{j^2}{\sigma}} \quad \textbf{(II.25)}$$

II.3.2. Moving boundary problem: Stefan Problem:

A Stefan problem is a moving boundary problem. In the context of melting/solidification problems, other terminologies for the moving boundary are free boundary, phase change boundary, melting front, solidification front, or phase change front. In its simplest formulation a Stefan problem is a linear 1D problem, where conduction is the predominant heat transfer mechanism and the convection term is not included in the energy equation. Since convection in neglected, there is no need to solve Navier-Stockes equations for the fluid flow motion. [14]

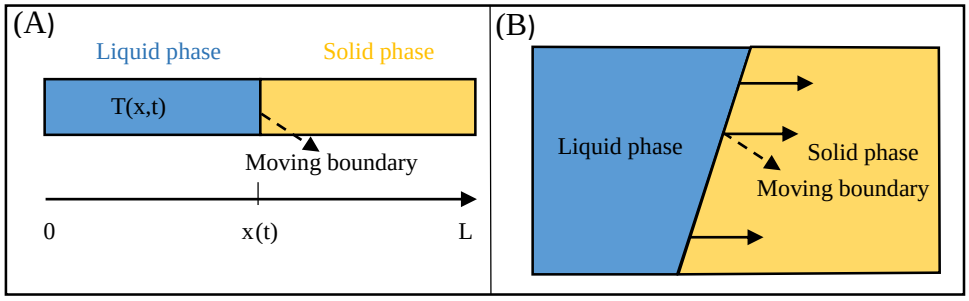

Fig.II.8. *Schematic representation of (A) 1D and (B) 2D Stefan problems.*

The governing energy equation, which is solved separately for solid and liquid phases, is as follows:

$$\boldsymbol{\rho_k C_{pk} \frac{\partial T_k}{\partial t} = \vec{\nabla}.\left(\lambda_k \vec{\nabla} T_k\right)} \qquad \textbf{(II.26)}$$

With $k = l, s$

In *Eq. (II.26)* the specific heat capacity C_p, the thermal conductivity $\boldsymbol{\lambda}$, and the density ρ, are assumed constant during the phase change. For a 1D problem, *Eq. (II.26)* is rewritten as:

$$\boldsymbol{\rho_k C_{pk} \frac{\partial T_k}{\partial t} = \lambda_k \frac{\partial^2 T_k}{\partial x^2}} \qquad \textbf{(II.27)}$$

The general form of heat balance on a solid-liquid interface, that is, the Stefan condition, is as follows:

$$\boldsymbol{\lambda_s \nabla T_s . n - \lambda_l \nabla T_l . n = \rho L v . n} \qquad \textbf{(II.28)}$$

Where n and v are the unit normal and velocity vector of the moving interface, respectively, and L is the latent heat per unit mass.

In the 1D form, the Stefan condition is defined as follows:

$$\boldsymbol{\lambda_s \frac{\partial T_s}{\partial x} - \lambda_l \frac{\partial T_l}{\partial x} = \rho L v} \qquad \textbf{(II.29)}$$

The *Eq. (II.29)* assembles the relations of the heat transfer rate in the solid and in the liquid, also the latent heat and velocity.

Bibliography

[9] Vasilios Alexiades, Alan D. Solomon, Mathematical modeling of melting and freezing processes, CRC press, Hemisphere Pub. Corp, 1992.

[10] Tadj, Hassani, Simulation numérique 2D instationnaire d'un problème de changement de phase sous l'effet de la convection naturelle, thèse de master 2020.

[11] https://en.wikipedia.org/wiki/Melting_point.

[12] Marianne Ostman, Pre-study of models and mapping physical modeling of scrap melting, Master thesis, 2006.

[13] Wu Y, Lacroix M, Numerical study of melting of scrap metal, Numerical heat transfer, Part A, 1993.

[14] https://www.sciencedirect.com/topics/engineering/stefan-problem.

[15] https://www.engineeringtoolbox.com/fusion-heat-metals-d_1266.html.

Chapter three:

Problematic, methodology and result's discussion

III. Chapter three: Problematic, methodology and result's discussion.

III.1. Problematic and methodology:

III.1.1. Preamble:

Before going to the role of electromagnetic fields in the melting by induction process, it seems very important to remind the basic notions and to outline the major effects that can be expected with applications of various EMF. Generally, application of electromagnetic fields is based on the two effects well-known for solid conducting objects:

- any electric current flowing in the conductor creates its own magnetic field
- motion of a conductor in the magnetic field generates electric current inside the conductor

The former effect allows one to create magnetic fields in space using arrangement of coils (also noted hereafter "inductors") of various geometry to which the electric potential $\Delta\Phi$, static or oscillating, can be applied. Alternatively, traveling (AC) magnetic field and continuous (DC) magnetic fields can be created with system of permanent magnets, which, in case of traveling field should be put in motion whereas for DC field they should be kept stationary.

With the static potential difference, the direct current, DC, circulates in the coil and creates the continuous (DC) magnetic field. Oscillating potential difference generates the alternated current (AC) in the coil and creates around its magnetic field, oscillating with the same frequency. According to the second effect mentioned above, if an electrically conductive load is placed near the coil, then the generation of the eddy current, heating, and the resulting effect of the electromagnetic force in the load depend on the character of the magnetic field, whether it is DC, monophase AC or polyphase AC.

Complete formulation of electromagnetic problem consists of four Maxwell equations-Faraday's law, Ampere's law, Gauss law for electric and magnetic field-completed with constitutive laws that relates electric charges, electric current with electric and magnetic fields and polarization, etc. For non-magnetic and non-polarizable materials this system of equation is simplified. Furthermore, modeling of electromagnetic field in application to material processing generally satisfies so-called "steady-state" or "electromagnetic" approximation. The latter assumes that the period of time required for electric charges to be redistributed within the media is significantly shorter than the characteristic time for variation of electromagnetic fields, i.e., no free (non-compensate) electric charges exist in conductors.

This chapter will focus mainly on the numerical resolution methodology adopted to solve the problem studied in this thesis. Indeed, the approached thematic constitutes a multidisciplinary crossroads mixing several physics: fluid mechanics, heat transfer and electromagnetism. In many cases, the production of traditional or new materials involves a melting phase at high temperature. This fusion step intended to produce the reaction or the homogenization in the liquid phase of the various constituents is decisive with respect to the properties of the material. The same applies to the solidification phase, possibly with simultaneous shaping during which the characteristics of the material freeze, sometimes irreversibly. Mastering and controlling the

melting and solidification processes are very delicate, especially when, to obtain precise properties, very strict purity and composition criteria are required.

III.1.2. Use of monophase AC magnetic field: magnetic pressure and heating:

Let the electric current which circulates in the coil oscillate with the angular frequency $\omega = 2\pi f$, in other words it changes periodically its direction in the coil. Magnetic field around each coil oscillates with the same frequency and its intensity decreases with the distance to the coil, resulting magnetic field in space is a superposition of standing waves. Oscillating magnetic field seen by the electrically conductive load generates in the latter oscillating eddy current that also creates magnetic field. Superposition of the phase shifted oscillating fields may result in "zeroing" of the magnetic field inside the load. A characteristic thickness inside the load within which the intensity of the magnetic field rapidly decreases is known as skin depth, and is defined with *Eq.(III.1)*.

$$\boldsymbol{\delta_m = \sqrt{\frac{2}{\mu_m \sigma \omega}}} \qquad \textbf{(III.1)}$$

Interaction of the eddy current and the magnetic field inside the load leads to the appearance of the Lorentz force composed of the constant mean value and the oscillating part, the mean value is oriented inside the load and tends to "squeeze" the load. It can be shown that for the cylindrical inductor and the load, with both of infinite lengths, the mean component of the Lorentz force is perpendicular to the load surface (*Fig. III.1*).

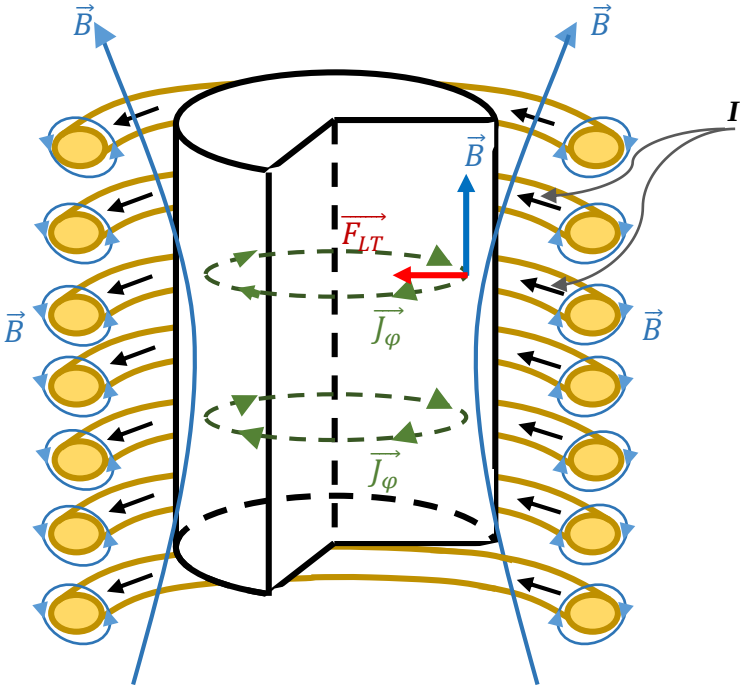

Fig.III.1. *With use of the monophase AC current in the coil: magnetic fields penetrate in the load over the distance δ_m (eq. (III.11)), the eddy current is mainly generated there. The averaged in time Lorentz force is directed perpendicularly to the surface of the load and plays the role of a magnetic pressure.*

In reality, finite dimensions of the load (or inductor) lead to the non-uniform intensity of magnetic field along the surface of the load that make the irrotational part of the electromagnetic force, $(B.\nabla)B$, non-zero, i.e., driving force appears in the load as well and affect fluid motion. Magnetic pressure can compete with gravity and may serve for making the levitation. However, the primary desired effect in industry is the heating which is produced in the load, according to the mainly within the skin depth.

III.1.3. Problem at hand

The object of this study is the electromagnetic modeling of an oven, cylindrical, in their almost-real environment. The approach adopted in this work is essentially based on the study of the effect of the application of an electromagnetic field generated by an external inductor on the melting process of a chosen pure material Tin (*Sn*), in terms of thermal field, dynamics and evolution of the melting front. To do this, an unsteady axisymmetric 2D two-phase numerical model based on the enthalpy approach, which resolves both: mechanical flow coupled to Maxwell's equations, energy, and phase change, was developed to simulate the whole phenomenon of fusion by Joule effect with the variation of several parameters.

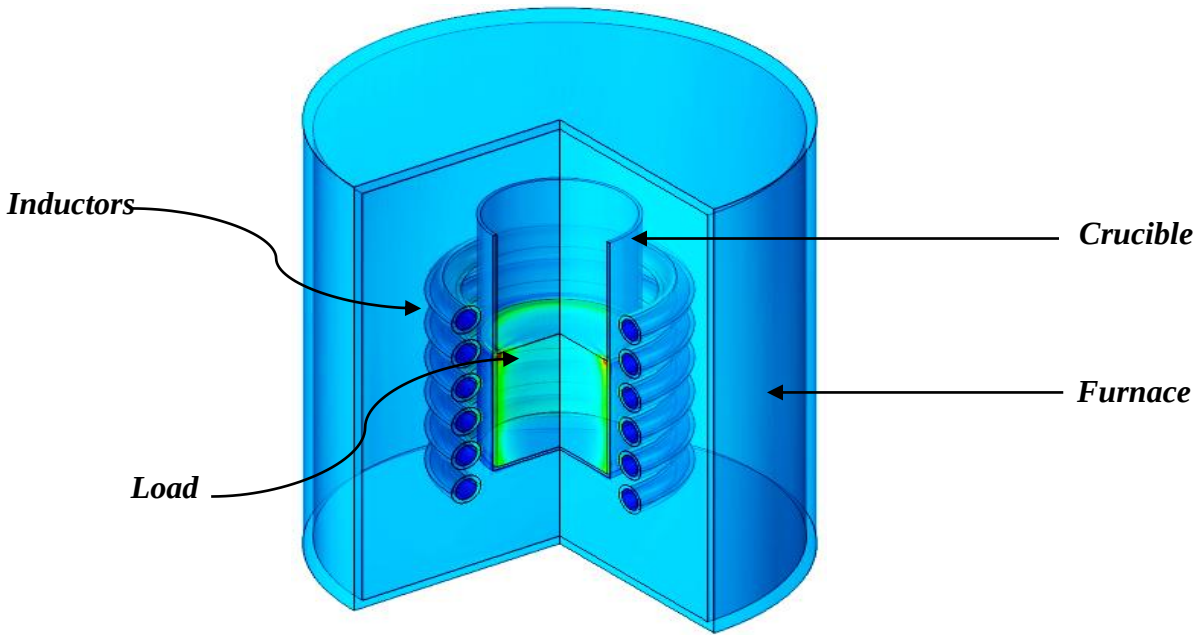

Fig.III.2. *System studied composed of an Aluminum furnace contains a crucible of Glass filled with a pure Tin material (Sn), characterized by a melting temperature (Tm = 232°C) and a coil of copper used as a source generating a magnetic field and cooled by water flow.*

III.1.4. Description of the system concerned:

The furnace is an aluminum cylindrical shape with a height $H_f = 600mm$, a diameter $D_f=596mm$ and a thickness $e_f=8mm$, inside the furnace we have the crucible lifted by $g=200mm$ from the bottom of the furnace, it is made of glass with a height $H_c=250mm$, a diameter $Dc=128mm$, and a thickness of $e_c=3mm$, this crucible is partially filled of the Tin charge with $H_t=120mm$. the electromagnetic inductor is a copper serpentine of six torus in surrounding the Tin charge, with diameter $d_o=28mm$. In order to cooling the inductors, we passed through the serpentine water flow with diameter $d_i=20mm$.

III.1.5. Model description and numerical details:

Since the problem at hand requires the resolution of several systems of non-linear partial differential equations (PDEs) with a relatively high degree of difficulty, the use of software adapted to this type of situation is essential for the resolution. Indeed, we leaned towards the COMSOL software for the numerical simulation because of its huge library of physical resolution models, especially for the electromagnetic/fluid mechanics coupling, as well as its simple, clear and explicit post-processing interfaces. The numerical model adopted in our study consists of a set of equations, boundary conditions and initial conditions, adapted to the problematic treated (electromagnetism, fluid mechanics, heat transfer and phase change). All of this is defined on a geometry decomposed into subdomains and limited by boundaries. The development of a simulation with COMSOL Multiphysics includes first the physical description of the problem, then the implementation of this model, and finally the verification of the results obtained by previous works if they existed or with experimental data [16]. The implementation phase consists of five steps:

III.1.5.1. Geometry (domain of study):

COMSOL Multiphysics provides a tool for designing 1D, 2D and 3D geometries. The geometry is described by a set of points, curves and surfaces. It is the basis for generating the mesh. [16]

For the geometry of our project, we start by drawing rectangles with different sizes and positions. Then we use the '*difference*' function between the rectangles to complete the shapes of the furnace and crucible, then we draw a rectangle that represents the study load, and create an inductor with '*difference*' function between two circles Finally we copy this inductor geometry five times on the same vertical axis.

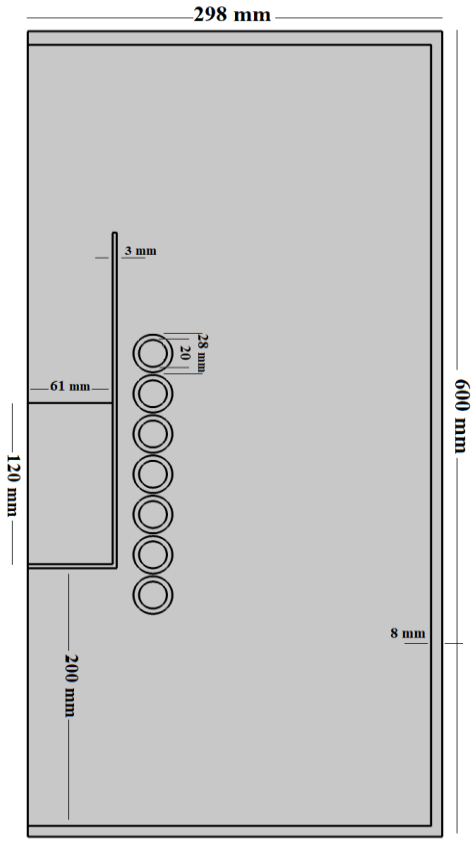

Fig.III.3. *2D axisymmetric geometry of the system.*

III.1.5.2. Physics:

In this step, the physical properties of the equations as well as the initial conditions are defined on the geometry, while the boundary conditions are defined on the external boundaries with respect to the study domain. To achieve this, three physics were used:

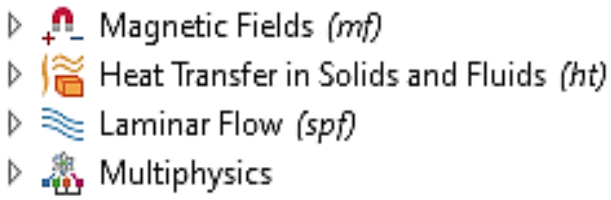

Fig.III.4. *The physics chosen in the simulation.*

- **Physics AC/DC Magnetic field:** AC/DC physics is used to calculate electric and magnetic fields in static low frequency systems. Indeed, this physics uses a complete vector formulation to solve the system under study. The magnetic field sub-interface, which is part of AC/DC physics, is used to calculate the magnetic field and current distributions induced in around conductors and magnets. Stationary analysis, frequency domain and time

domain modelling are supported in 3D. It is important to note that this interface solves Maxwell's equations using the magnetic vector potential and in the case of coils, the electric potential scalar as dependent variables [17]. In this physics the COMSOL solves:

Ohm law: $\vec{J} = \sigma\overrightarrow{E_r} = \sigma(\vec{E} + \vec{u} \times \vec{B})$

Induction equation: $\frac{\partial \vec{B}}{\partial t} = \vec{\nabla} \times (\vec{V} \times \vec{B}) + \lambda \nabla^2 \vec{B}$

Lorentz force: $\vec{F} = \vec{J} \times \vec{B}$

Denoting the electrical conductivity of which we will take $\sigma = 3.6 \times 10^6\ S/m$.

Magnetic induction field $B = \mu_0 \mu_r H$, with μ_r representing the relative permeability equal to "1", μ_0 denotes the permeability for vacuum equal to "$4\pi.10^{-7} SI$".

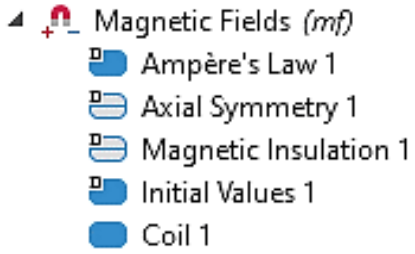

Fig.III.5. *The Magnetic field physic chosen in the simulation.*

- **The second physics is «Laminar Flow»:** is used to calculate the velocity and pressure fields in a laminar flow regime. A flow will remain laminar in confined cavities as long as the Rayleigh number is below a certain critical value. Indeed, for higher Rayleigh numbers, disturbances tend to increase and cause a transition to turbulence. This critical Rayleigh number depends on the configuration studied. [18]

The coupled conservation equations describing the flow are the Navier-Stokes equations. Taking into account the assumptions mentioned above, these equations are expressed as follows:

Conservation of mass equation: $\frac{\partial \rho}{\partial t} + \nabla.(\rho \boldsymbol{u}) = \mathbf{0}$

Conservation of momentum equation:

$$\rho \frac{\partial u}{\partial t} + \rho(u.\nabla)u = \nabla.[-pI + u(\nabla u + (\nabla u)^T) - \frac{2}{3}\mu(\nabla u)I] + F$$

Where $\vec{F} = \rho g \beta \Delta T \vec{k} + \vec{j} \wedge \vec{B}$ are the volume forces applied to the load. Strongly coupled with previous physic chosen (AC electromagnetic)

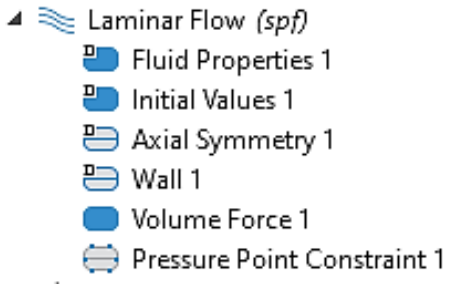

Fig.III.6. *Laminar flow physic chosen in the simulation.*

- **The third physics is "Heat Transfer in fluid" with implicit phase change physics:** The fluid heat transfer interface is used to model heat transfer in fluids by conduction, convection and radiation. A fluid model is active by default on all domains. All features to include other domain types, such as a solid domain, are also available.[19], The temperature equation defined in the fluid domains corresponds to the convection-diffusion equation which may contain additional contributions such as heat sources.

$$\rho C_p \frac{\partial T}{\partial t} + \rho C_p V.\nabla T = \nabla.(k\nabla T) + \frac{J^2}{\sigma}$$

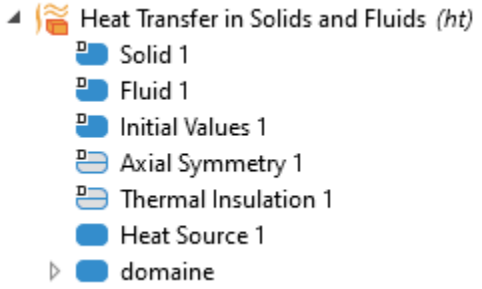

Fig.III.7. *Conjugate Heat Transfer physic chosen in the simulation.*

III.1.5.3. Meshing:

It corresponds to the spatial discretization of the geometry. The meshes are of polygonal in 2D (triangle or quadrangle) and polyhedral in 3D (tetrahedron, prism, brick, or cube). In some 3D cases, the domain is difficult to discretize exactly. The mesh is generated automatically or imported, or set up by the user who can choose the type of mesh. The number of nodes, the number of unknown variables and the order of the interpolation functions determine the number of degrees of freedom (DOF) of the problem to be solved. The larger the number of meshes, the more memory the problem needs on the machine. The weak point of COMSOL Multiphysics would perhaps be in this step, because this code does not offer an adaptive mesh for temporal calculations, and the meshes are isotropic whereas for a problem such as ours, an anisotropic mesh would be preferred.

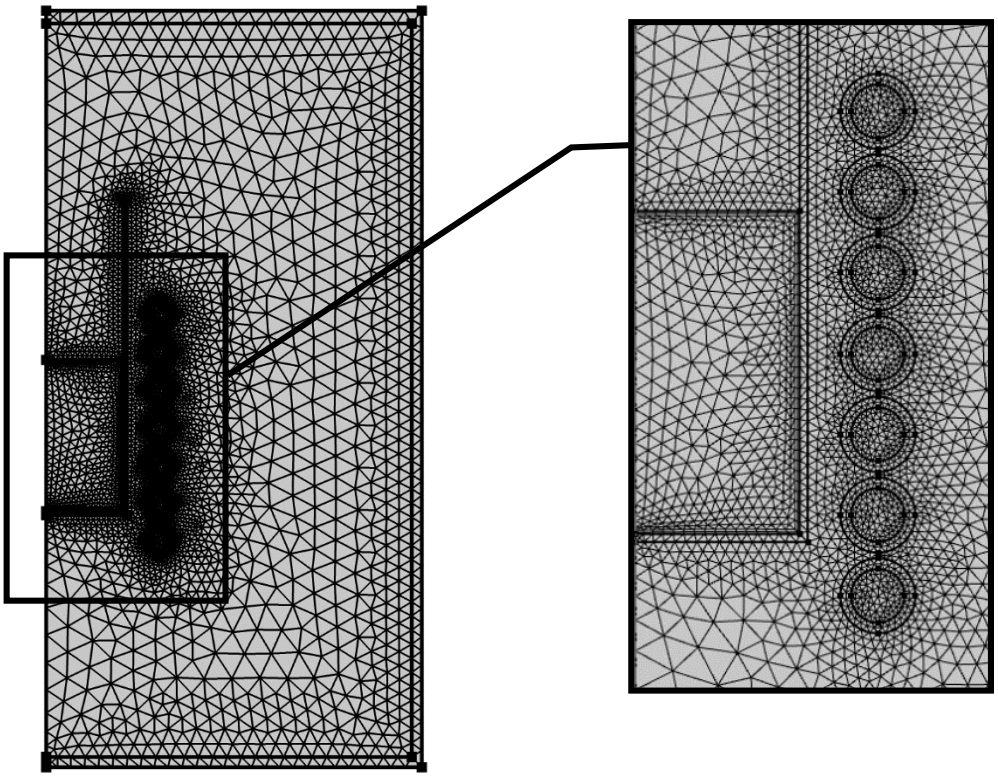

Fig.III.8. *2D axisymmetric mesh of the system.*

The mesh adopted in this work is a *"finer"* mesh (see *Fig.III.8*), produced automatically by commercial software "COMSOL Multiphysics". The entire mesh consists of *7243* domain elements, and *834* edge elements. It is observed that the extra thin mesh is concentrate at the edge of the charge and around the inductors, this thin mesh is presented to define clearly the physics in the boundary layer, limit condition and the magnetic skin-depth effect in the charge.

III.1.5.4. Choice of Solver:

The user can choose a type of analysis (stationary, temporal, modal or parameterized) and the resolution algorithm. COMSOL Multiphysics offers solvers based on two types of solution methods:

- Direct solvers which are accurate and fast but require a lot of memory.
- Iterative solvers, whose convergence is subject to certain conditions, less accurate but more economical in memory.

There is no solver that is more accurate than another, since all solvers should meet the same convergence criteria discussed.

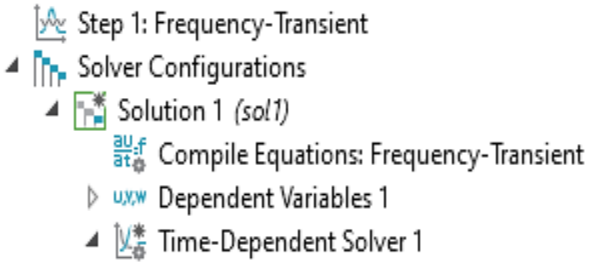

Fig.III.9. *Solver chosen in the simulation.*

III.1.5.5. Post-treatment:

This step is reserved for the analysis of the results. The graphical interface of COMSOL Multiphysics offers the possibility to see the results on the whole geometry, on sections or on individual elements. Spatial integration of any variable is also available, as well as the possibility of exporting them in different formats.

III.1.5.6. Initial and boundary conditions:

Once the domain is meshed and the physical properties of the materials are defined (see *Table.III.1*), the initial and boundary conditions, thermal and magnetic boundary conditions

Table.III.1. *Physical properties of Tin "Sn".*

Properties	***Symbols***	***Values***	***Unit***
Heat capacity at constant pressure (solid/liquid)	C_p	*200/220*	$[J\ /\ Kg.K]$
Thermal conductivity (solid/liquid)	λ	*60/30*	$[W/(m.K)]$
Coefficient of expansion at constant pressure	β	2.2×10^{-5}	$[1/K]$
Conductivity electrical	σ	3.6×10^{6}	$[S/m\ ]$
Dynamic viscosity	μ	*0.006*	$Pa.s$
Ref. pressure	P_0	*100*	*[Pa]*
Density	ρ	*7070*	$[kg/m^3]$
Frequency	$Freq$	*1000*	*[Hz]*
Surface current	J_0	*500*	*[A/m]*

- **Initial conditions: at *t = 0 [s]***

- Velocity range: $u_x = u_y = u_z = 0\ [m/s]$
- Pressure: $P = 0\ [Pa]$

- Potential magnetic vector: $A_0 = 0\ [T]$
- The furnace is considered Adiabatic: $\frac{\partial T}{\partial u}\Big|_{normal} = 0$

➢ **Boundary conditions:**

- Thermically isolation: $n.(k\nabla T) = 0$
- Pressure stress: $P_0 = P_{ref} = 100\ [Pa]$
- Water temperature: $T_{water} = 15\ ℃$

III.1.5.7. Calculation assumption:

The proposed model is based on the following assumptions:

- The problem is transition three-dimensional.
- The flow is considered laminar.
- The material is in the liquid state considered as an incompressible fluid $\rho = cst$.
- The Boussinesq approximation is used in the calculation of natural convection.
- The heat transfer by radiation is neglected.
- The process of heating is carried out under a secondary vacuum in order to avoid all heat losses by convection.

III.1.6. Convergence of solution:

The numerical method consists in interpolating the solution on a discretization of the geometry (mesh). A numerical solution is acceptable when the convergence criterion is established, i.e., when the numerical result is very close to the exact solution. That is precisely unknown, it is only accessible in certain cases for simple geometries. So, an error estimate is constructed from a second order Taylor development of the differential operator of the system of equations. Convergence is achieved when the value of the estimated error is below a certain value. Error estimation only makes sense in the case of a non-linear and/or temporal system of equations, because for a linear case the solution corresponds to the inversion of the system matrix without verification:

- The error for the non-linear case is $err = \sqrt{\left(\frac{1}{N}\sum_i \left(\frac{|E_i|}{W_i}\right)^2\right)}$,where N is the number of nodes, E is the error estimate, and W is the weight of each node (equal to 1 by default). This value must be less than a user-defined factor (its default value is 10^{-6}).
- For a temporal calculation, the solution must satisfy the criterion $\sqrt{\left(\frac{1}{N}\sum_i \left(\frac{|E_i|}{A_i+R|U_i|}\right)^2\right)} < 1$, each time step, where A_i is the absolute tolerance (default value 10^{-3}), and U_i is the relative tolerance (default value 10^{-2}).

The convergence reflects the relevance of the numerical solution with the approximate solution of the model. The (numerical) quality of the obtained solution and its stability depend on the refinement of the mesh and the time step chosen to satisfy the CFL condition.

III.2. Result's discussions:

In this part, we present all the results obtained through the unsteady 2D axisymmetric numerical model adopted in our work. The purpose is to review, first of all its efficiency in solving the set of partial differential equations to be solved (Navier stokes, Maxwell, energy, phase change and continuity). The focus will be on the effects of induction heating created by electromagnetic stirring on the dynamic and thermal configuration in a cylindrical crucible,

We will present the results in two types, the first consists of descriptive 3D graphics evolution of magnetic field, hydrodynamic field, temperature field and finally front of phase change behavior. Then, the second part will present as a 2D graphics, the isothermal contours, the liquid fraction and the velocity. To understand the phenomena of induction heating it is useful to analyze and compare this data.

III.2.1. Magnetic field distribution

As previously detailed, the cylindrical inductor possesses seven winding and is located around the crucible at $R_i = 9\ cm$. Its height is $H_{ind} = 18\ cm$. This inductor is fed by a mono-phase AC current with a frequency $f = 1\ kHz$. The numerical results obtained for the magnetic field distribution in terms of 2D axisymmetric evolution as well as it's modulus $\|\vec{B}\| = \sqrt{\overrightarrow{B_r^2} + \overrightarrow{B_z^2}}$ in different z-positions were taken in the load at vicinity of the inner surface of the crucible ($R = 6\ cm$) for applied electric currents ($J_0 = 500\ A$), are shown in *Fig. III.10*. The results presented in the *Fig.III.10-a*, show that the magnetic field can reach *25 mT* beside the inductor, whereas in the charge it is arround *19.6 mT* (see *Fig.III. 10-b*). The latter clearly shows that the distribution of the magnitude field density within the charge, namely in the magnetic skin is almost constant, except for a small variation between the central part and the two edges which does not exceed *2 mT*.

The estimate of thickness of electromagnetic skin depth due to the effect of frequency through the pure metal (Tin) was based on theoretical analysis developed previously for the same configuration in the case of a single-phase induction system:

$$\boldsymbol{\delta = \sqrt{\frac{2}{\mu\sigma\omega}} = \sqrt{\frac{2}{4\pi \times 10^{-7}\ (\mathrm{H.m^{-1}})\ 3.4\ 10^{6}(\Omega.m)^{-1}(2\pi 1000 Hz)}} = 8.4\ mm}$$

Where μ is the permeability ($\mu = 4\pi \times 10^{-7}\ H.m^{-1}$) and σ the electrical conductivity ($\sigma = 3.6 \times 10^{6}\ \Omega^{-1}.m^{-1}$) of tin.

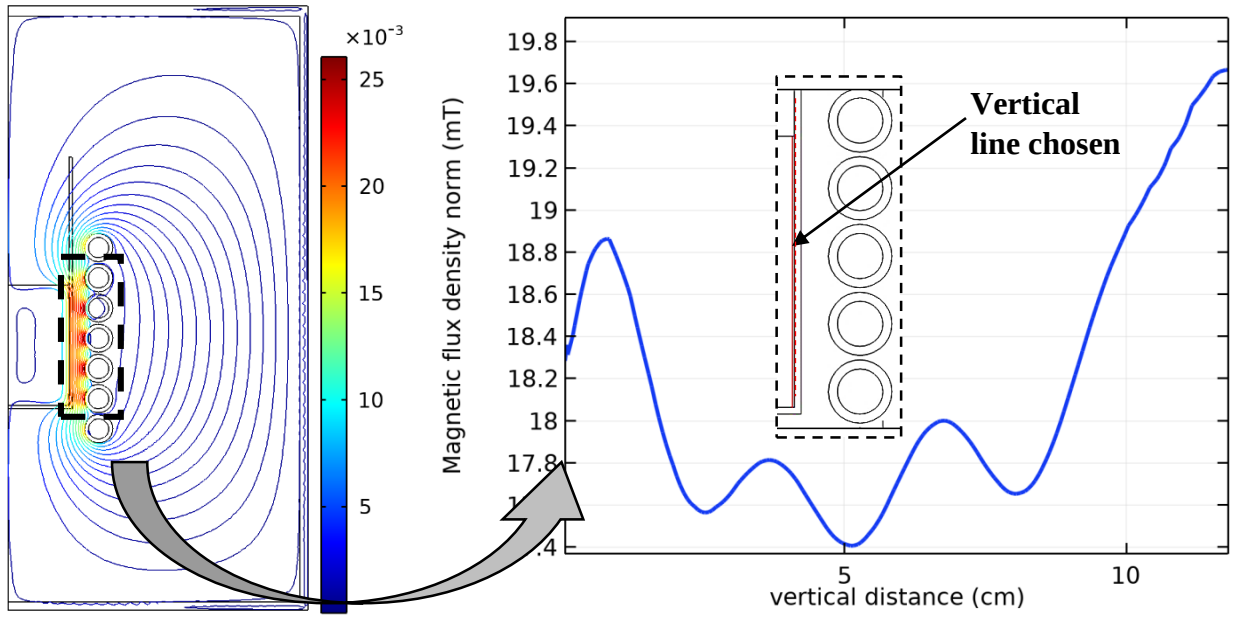

(a) ***(b)***

Fig.III.10. *Distribution of the magnetic flux density on the chosen vertical line in the vicinity of the internal surface of the electromagnetic inductor.*

III.2.2. Buoyancy and Lorentz forces distribution:

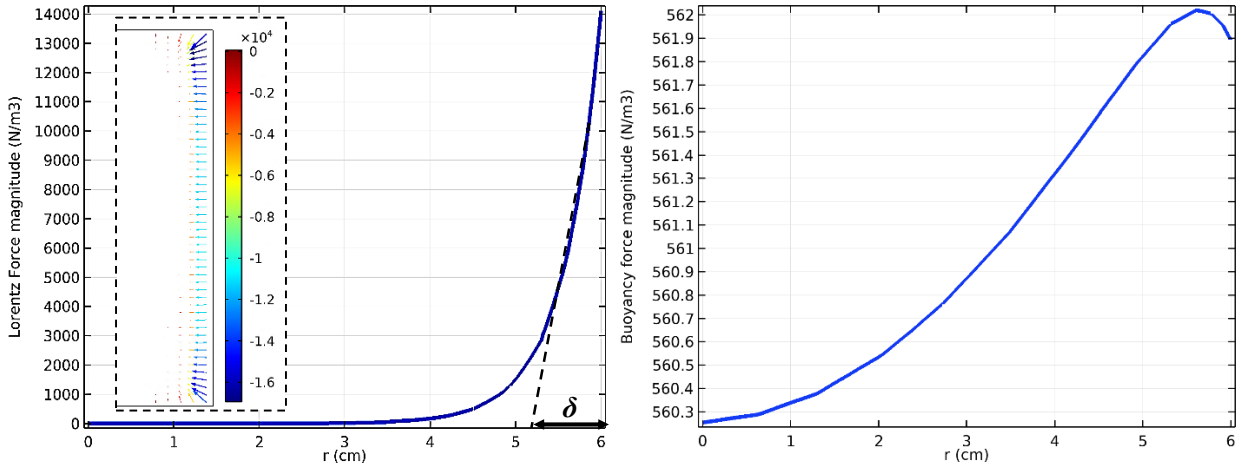

(a) ***(b)***

Fig.III.11. *Spatial evolution of volume forces magnitude in the radial direction (z = 26.3 cm, and r varies between 0 and 6 cm). Results obtained for the condition: f = 1 kHz and I = 500 A. (a) Lorentz force and (b) buoyancy force.*

According to the melt configuration which corresponding to an electrically conducting liquid in a regular cylinder of radius R and height H subject to an axisymmetric magnetic field $\vec{B} = \vec{\nabla} \times \vec{A}$ with angular frequency ω; amplitude B_0 and the vectorpotential $\vec{A}(0\,\vec{e}_r, A_\varphi \vec{e}_\varphi, 0\,\vec{e}_z)$ such that

$\vec{A}(r,\varphi,z) = 0.5B_0 r cos(\omega t)\vec{e}_\varphi$. Under the assumptions above the induced current is $\vec{J} = (0\ \vec{e}_r, 0.5\sigma\omega B_0 r cos(\omega t)\vec{e}_\varphi, 0\ \vec{e}_z)$. The effective electromagnetic force is approximated analytically as $\vec{F}_{LT} = \vec{J} \times \vec{B} = \left(J_\varphi B_z \vec{e}_r, 0\ \vec{e}_\varphi, -J_\varphi B_r \vec{e}_z\right)$.

As expected, the component $\vec{F}_\varphi$ has a zero-time (or φ) average. In addition, all terms are proportional to $cos(\omega t)$, which are periodic functions of *t*, as can be discerned in the *Fig.III.11-a*. Thus, both $\overrightarrow{F_r}$ and $\vec{F}_z$ have a nonzero average that decreases exponentially with r and exhibits the classic skin depth of thickness δ of about *8.4 mm*, (see *Fig.III.11-a*)**.** Clearly, the average of $\vec{F}_z$ is the driving force however is significantly negligible compared to $\vec{F}_r$ due to the low value of the radial component of the magnetic field $\overrightarrow{B_r}$; the average of $\overrightarrow{F_r}$ is a repulsive force, which affects the pressure distribution. It is important to mention that the radial component of Lorentz force is only activated in the magnetic skin.

Furthermore, the buoyant force $\vec{F}_{buoy} = \rho\vec{g}\beta_T\Delta T$, created by the temperature gradient existing during the melting process is shown in *Fig. III.11-b*. Apart from the viscous boundary layer, for which this force is relatively damped, this latter is almost constant ($F_{buoy} \approx 560\ N/m^3$) and can be considered as the effective dominate driving force in the liquid phase.

III.2.3. Temperature profiles:

In this part, the effect of electromagnetic induction on the behavior of the thermal field in terms of temperature contours and its corresponding thermal gradients at three selected representative time steps, was examined. The 3D temperature revolution as well as the corresponding temperature map at time *t = 2625 s*, are respectively presented in *Figs (III.12-a* and *b).* In addition, the temporal evolution of temperature on a selected vertical line located at (*r = 5 cm* and *z* varying between *26.3* and *32.3 cm*) for the instants (*2600*, *2625*, *2650* and *2675*s) is presented in *Fig. III.12-c*.

It is important to mention that the curves of the temperature temporal evolution presented in *Fig. III.12-c*, have the same behavior, which are characterized by a thermal gradient of about *2K* between the center part and the two edges (bottom and upper), respectively. This behavior can be explained by the no homogeneity of heating by induction due to the distribution of magnetic field presented previously in *Fig III.10-b*. The four-time steps have been selected to be representatives according to the phase change process. Indeed, the instant *2600s* represents the time where the sample was completely solid, however the instant *2625s* corresponds to the beginning of the melting stage in the upper part. The two last instants (*2650* and *2675s*) correspond the case of load completely liquid, where the temperature level exceeds the melting point and consequently the convection becomes relatively significant.

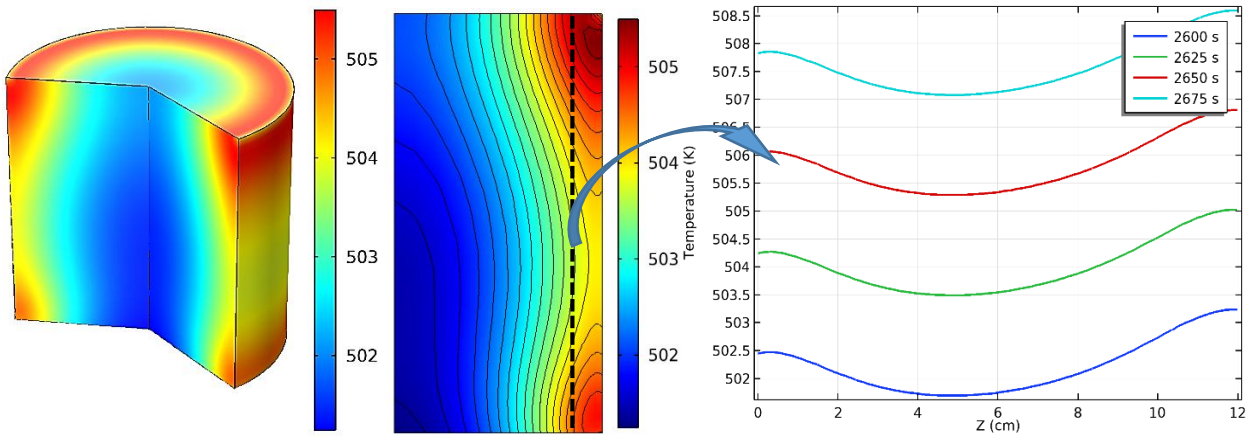

(a) ***(b)*** ***(c)***

Fig.III.12*. (a) 3D temperature revolution and (b) the corresponding temperature map at time t = 2625 s. (c) Temperature evolution for selected vertical line (r = 5 cm and z varying between 26.3 and 32.3 cm) at four selected representative time steps (2600, 2625, 2650, and 2675).*

As well reported in the literature, when a pure material is heated, at constant pressure, the phase change occurs always at a constant temperature, this latter is the melting temperature (T_m = *505K* in our case). At this melting point, both liquid and solid phases of the material co-exist. During the solid-liquid phase change, the melting point is usually defined by melting temperature only. In the case of pure metal, primarily in a solid state which is then slowly heated in a crucible until its completely melted, this heating curve is achieved by recording the change of the temperature at each point within the process over time. Indeed, the phase change process is characterized by an isothermal stage in which the temperature remains constant and equal to the melting temperature, and here both solid and liquid phases of the material coexist. In the beginning, the first liquid drops are hardly formed, these drops then grow until the solid phase around the melting point has completely disappeared, the metal is then completely melted. This isothermal plateau become larger as the heating is slower and the mass solidified is greater. Since melting is an endothermic phenomenon, latent heat is absorbed along this plateau. In order to examine the effect of electromagnetic induction heating on the temperature field in the load, the time course of the temperature of five selected points chosen on the same horizontal centerline is tracked and presented in *Fig.III.13.*

The figure *Fig.III.13* clearly shows that these points present the same temporal of thermal behavior. Indeed, all curves indicate that the heating carried out in a linear manner which confirms the dominance of the conductive mode, thereby including the phase change solid-liquid. It is very important to mention that these curves clearly indicate the completely absence of the isothermal plateau during the melting stage which may be explained by the faster heating resulted to the both high electrical current and frequency supplying the electromagnetic inductor which does not allow enough time to this plateau to be occur.

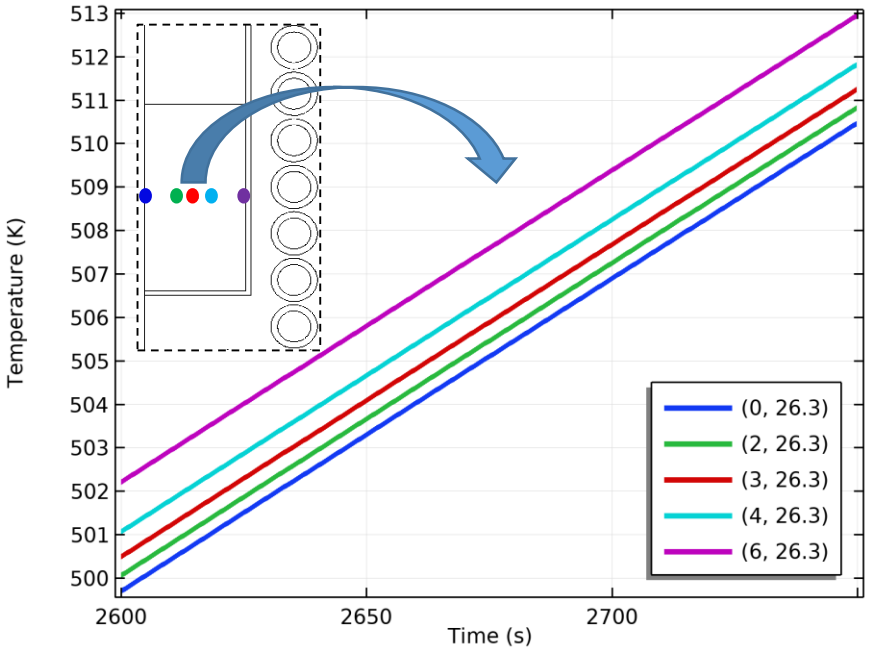

Fig.III.13. *Time-evolution of temperature for five selected points, located in the same horizontal middle line: point 1 (r = 0 cm, z = 26.3 cm), point 2 (r = 2 cm, z = 26.3 mm) and point 3 (r = 3 cm, z = 26.3 cm), point 4 (r = 4 cm, z = 26.3 cm) and point 5 (r = 6 cm, z = 26.3 cm).*

III.2.4. Liquid fraction

In the light of the previous analysis between the four cases in terms of temperature behavior, we have shown the need to study the effects related to the shape of the melting. Melting starts when the first drop is formed in the solid zone and continues until there is no trace of any solid in the system (see *Fig. III.12*). In Figure **(***Fig.III.14*) below, four different instantaneous color maps of the progress of the melting process over time show an exposition of the numerical simulations results during the process.

At *t = 2610 s*, temperature of the upper right corner is the first temperature in the sample to exceed above Tm (see *Fig. III.14-a*). The melting starts from the upper right corner where the sample is mainly liquid. A descending curved melting front appears on this side under the effect of the thermal gradient. Electromagnetic induction also has a strong effect on the shape of the solidification front, as illustrated in *Fig. III.10-b*. However, in the *Fig. III.14-b*, which corresponds to the instant *2625 s*, we can easily observe the appearance of a second melting front in the lower right corner, which indicted a delay of about *15 s* between the two corners due to the nonuniformity distribution of induced current, as was previously detailed.

At *t = 2675 s*, the map clearly shows the progression of the solidification front from right to left. The shape of the melting front tends to be parabolic. The curvature of the melting front is caused by the thermal gradient derived from the induced current distribution. It is important to note that both the curvature of the melting front and its own forward velocity are relatively accentuated due to the effect of convection activated in the right side, as the melting proceeds.

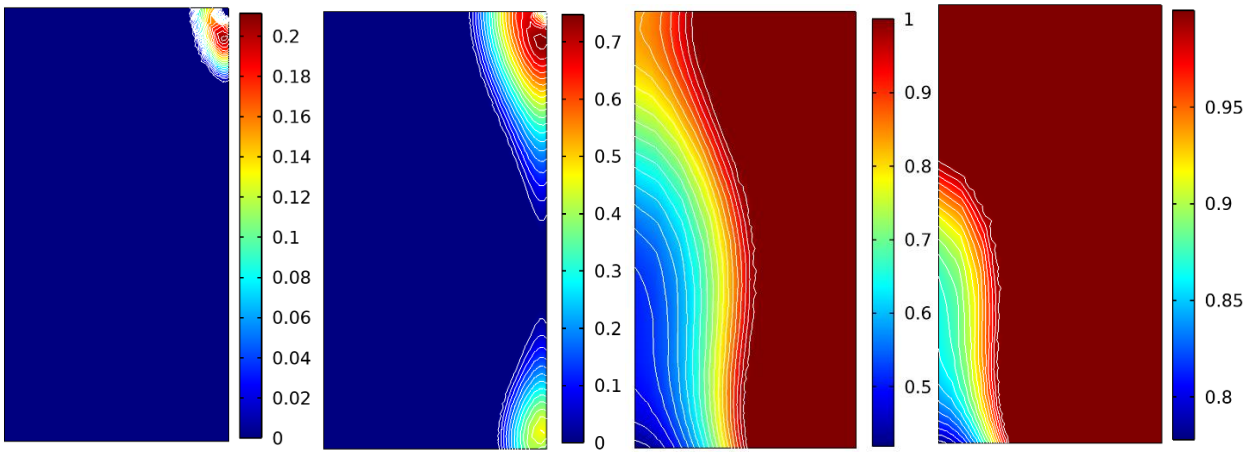

(a) t = 2610 s ***(b) t = 2625 s*** ***(c) t = 2675 s*** ***(d) t = 2685 s***

Fig.III.14. *Solid-liquid front positions at different times during the melting process. The color bar gives the liquid fraction.*

Lastly, at *t = 2685 s*, the convection becomes significantly strong, and the liquid volume increases in one hand, and melting fronts progress, reducing the solid region in the other. As expected, the last solid at this instant is located in the bottom left corner of the sample.

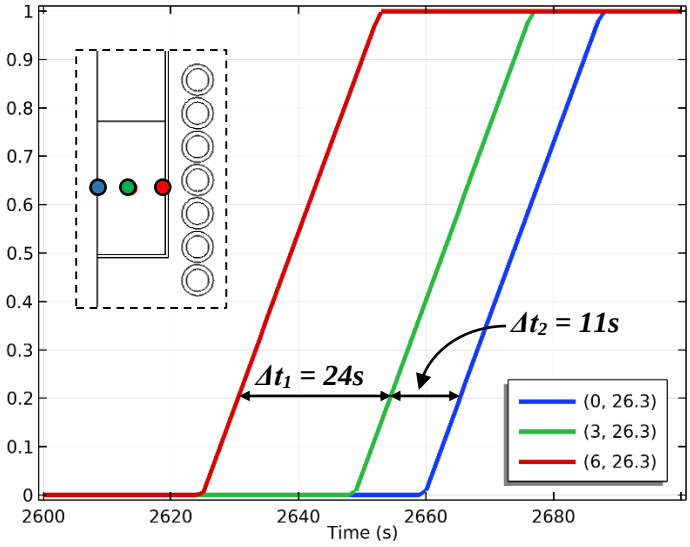

Fig.III.15. *Time-evolution of liquid fraction for three points, located in the same horizontal middle line: point 1 (r = 0 cm, z = 26.3 cm), point 2 (r = 3 cm, z = 26.3 mm) and point 3 (r = 6 cm, z = 26.3 cm).*

Furthermore, in order to give more details about the melting by electrmagnetic induction, we have followed the history of the liquid fraction of three different points: point 1 (*r = 0 cm, z = 26.3 cm*), point 2 (*r = 3 cm, z = 26.3 mm*) and point 3 (*r = 6 cm, z = 26.3 cm*), located in the same horizontal middle line of the sample, presented in *Fig.III.15.*

Fig.III.15 shows the time-evolution of liquid fraction for each point selected. It is easy to note that due to the increase of temperature in these points, which becomes above than the melting temperature (T_m = *505 K*), the liquid fraction has increased from initial value f_l = 0 to *1* in *29s* for both three points (*1*,*2* and *3*), which corresponding to the melting progress. However, although the distance between the three selected points is identical, the time difference between the onsets of melting between these points has a tendency to be reduced (from *24 s* to *11s* in this level for example) due to the increase in the advancement velocity of the liquid-solid interface.

III.2.5. Velocity profile

The ability of our 2D axisymmetric model to predict the velocity after melting within the sample is shown in *Fig. III.16*. The velocity fields are represented as colored magnitude levels vectors, while the streamlines are represented by black lines. The purpose of this part is to verify the effect of the existing temperature gradient on the velocity field by examining the effect of the buoyancy force to create a motion within the load.

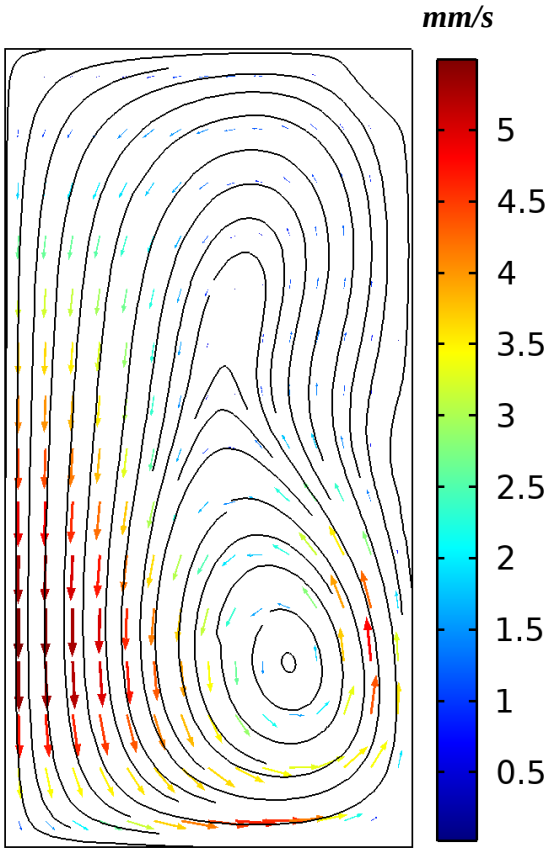

Figure III.16. *Two-dimensional spatial instantaneous evolution of dynamic field (numerical simulation). The black lines correspond to the streamlines and volume vectors are the velocity forces. Results obtained for the condition: f = 1kHz and I = 500A.*

The results show clearly that when the sample becomes completely liquid, we can distinguish mainly a one vortex appears and spreads over the entire cavity having a center located in the middle-lower part of the sample near the hottest wall. In the present configuration, where the buoyancy forces are thus dominant compared with the Lorentz in the vertical direction. The corresponding Reynolds number based on the maximum velocity (u_{max} = *5 mm/s*) is:

$$\boldsymbol{Re = \frac{u_{max}(u = 0.005 m/s)\left(\frac{H^2}{D}\right)}{\nu} = 2247}$$

Where *v* is the kinematic viscosity of pure tin in liquid state ($v = 2.67\ 10^{-7}\ m^2\ s^{-1}$).

The value of Reynolds indicates that the melt flow regime is likely to be laminar for the case of cylindrical geometry.

Bibliography

[16] Djeridane et Bourahla, Modélisation numérique 3D instationnaire de la convection forcée par brassage électromagnétique dans une cavité parallélépipédique, Thèse de Master, 2020.

[17] User's guide COMSOL, «AC/DC Module», 2018.

[18] User's Guide COMSOL, « Microfluidics Module », 2018.

[19] User's guide COMSOL, «Heat transfer module», 2018.

Conclusion:

During this End of Study Project (ESP), first of all we were able to understand the preliminary basic notions related to the phenomena involved in the process of melting of pure metal (tin), and highlight the main numerical approaches used to deal with this multidisciplinary phenomenon. Indeed, the work carried out in this master's thesis had as objectives the numerical simulation through a commercial software COMSOL, simultaneously allowing the resolution and the complex coupling between the governing equations: Maxwell, Navier stokes and energy on the one hand and the specific phase change equations, on the other hand. The results obtained numerically allowed us to determine the effect of electromagnetic induction on the whole melting process of this chosen material in terms of thermal field, dynamic field, as well as the evolution of the solid-liquid interface (melting front).

In the light of the results obtained numerically from the simulation of such a complex phase change phenomenon with axisymmetric electromagnetic induction heating by imposing a high frequency of *1 kHz* and monophase alternating current of *500 A*, the model has shown its effectiveness in solving all the systems of complex equations cited above, for predictive purposes of the spatiotemporal evolution of the melting front.

It is important to mention that this work requires a parametric study dealing with the main factors that have a direct effect on the phase change process as for example the changing of: frequency, the current configuration, the geometric ratio and the physical properties in terms of the Prandtl number, in order to identify the impact of the influence of these factors and optimize a better compromise between them. Once again, the results are very conclusive, with however a relevant questioning about the absence of the phase change thermal plateau which remains to be explained.

Unfortunately, the major drawback of this work results in the lack of validation with the experimental work carried out in this context, and this due to the fact that the simulation carried out is limited to the 2D axisymmetric case only, which represents a real constraint for the validation.

Finally, our work is only an initiative study in a rather complex field, hoping that it will be a reliable basic bibliographic reference for other more in-depth studies later.

ملخص: يعد تطوير المواد مصدر قلق مشترك من قبل الباحثين في مجال علم المواد والشركات الصناعية الذين لديهم اهتمام بتلبية الاحتياجات الجديدة للتقنيات الحديثة. في كثير من الحالات، ينطوي تطوير المواد التقليدية أو الجديدة على مرحلة انصهار عند درجة حرارة عالية. تهدف هذه خطوة إلى إنتاج التفاعل المتجانس في الطور السائل للمكونات المختلفة، وهي خطوة حاسمة فيما يتعلق بخصائص المادة.

غالبًا ما يكون الذوبان، بغض النظر عن طريقة إنتاج الحرارة، هو سبب تدهور نقاوة العناصر الأساسية التي تشكل المادة النهائية. في الواقع، تتفاعل هذه العناصر في الحالة السائلة وعند درجات الحرارة العالية من خلال التفاعلات الفيزيائية والكيميائية مع جدران البوتقات اللازمة لاحتوائها وايضا يتضمن هذا بشكل عام فرض حركة تقليب على المعدن أثناء تغيير المرحلة الصلبة السائلة. ومع ذلك للتقليب العديد من المزايا على الهيكل المعدني، فإنه لا يخلو من العيوب فيما يتعلق بنقاء المادة المنتجة عن طريق إدخال عناصر التقليب في الجزء السائل.

Abstract: Materials development is a common concern for materials scientists and industrialists who have an interest in meeting the new needs of new technologies. In many cases, the development of traditional or new materials involves a high temperature melting phase. This step is intended to produce the homogeneous reaction in liquid phase of the different components, and is a critical step with respect to the properties of the material.

The melting, whatever the mode of heat production, is often at the origin of the degradation of the purity of the basic elements which compose the final material. Indeed, these elements interact in the liquid state and at high temperature by physical and chemical reactions with the walls of the crucibles necessary to contain them, which also usually involves imposing a stirring motion on the metal during the change in solid-liquid phase. However, the stirrer has many advantages over the frame, it is not without disadvantages regarding the purity of the material produced by the introduction of the stirring elements in the liquid part.

Résumé : L'élaboration de matériaux est une préoccupation commune aux chercheurs dans le domaine de la science des matériaux et aux sociétés industrielles qui ont le souci de répondre aux besoins nouveaux des technologies modernes. Dans de nombreux cas, l'élaboration des matériaux traditionnels ou nouveaux, fait intervenir une phase de fusion, à température élevée. Cette étape de fusion destinée à produire la réaction homogène en phase liquide des divers constituants est déterminante vis à vis des propriétés du matériau.

La fusion, quel que soit le mode de production de chaleur est très souvent à l'origine d'une dégradation de la pureté des éléments de base qui constituent le matériau final. En effet ces éléments à l'état liquide et à température élevée réagissent par le biais de réactions physicochimiques avec les parois des creusets nécessaires pour les contenir.

Ceci implique généralement d'imposer un mouvement de brassage au métal lors du changement de phase solide-liquide. Cependant, si le brassage présente beaucoup d'avantages sur la structure métallurgique, il ne va pas sans inconvénient vis à vis de la pureté du matériau élaboré, par l'introduction dans la partie liquide brassée d'éléments extérieurs.

END